This manuscript is the accepted version of the paper:

HDPE geogrid-residual soil interaction under monotonic and cyclic pullout loading, Geosynthetics International, Vol. 27, Issue 1, pp. 79-96, https://doi.org/10.1680/jgein.19.00057

HDPE geogrid-residual soil interaction under monotonic and cyclic pullout loading

F. B. Ferreira[1], C. S. Vieira[2], M. L. Lopes[3] and P. G. Ferreira[4]

[1] Postdoctoral Researcher, CONSTRUCT-GEO, Faculty of Engineering, University of Porto, R. Dr. Roberto Frias, 4200-465 Porto, Portugal, Telephone: +351 225081286, Telefax: +351 225081446, E-mail: fbf@fe.up.pt (Corresponding author)

[2] Assistant Professor, CONSTRUCT-GEO, Faculty of Engineering, University of Porto, R. Dr. Roberto Frias, 4200-465 Porto, Portugal, Telephone: +351 225081586, Telefax: +351 225081446, E-mail: cvieira@fe.up.pt

[3] Professor, CONSTRUCT-GEO, Faculty of Engineering, University of Porto, R. Dr. Roberto Frias, 4200-465 Porto, Portugal, Telephone: +351 225081564, Telefax: +351 225081446, E-mail: lcosta@fe.up.pt

[4] Postdoctoral Researcher, CONSTRUCT-ViBest, Faculty of Engineering, University of Porto, R. Dr. Roberto Frias, 4200-465 Porto, Portugal, Telephone: +351 225083712, Telefax: +351 225081446, E-mail: pedro.gil.queiros@fe.up.pt

ABSTRACT: The understanding of soil-geosynthetic interaction under cyclic loading conditions is essential for the safe design of geosynthetic-reinforced soil structures subjected to repeated loads, such as those induced by road and railway traffic and earthquakes. This paper describes a series of large-scale monotonic and multistage pullout tests carried out to investigate the behaviour of a HDPE uniaxial geogrid embedded in a locally available granite residual soil under monotonic and cyclic pullout loading. The effects of the pullout load level at the start of the cyclic stage, cyclic load frequency and amplitude, number of cycles and soil density on the load-strain-displacement response of the reinforcement are evaluated and discussed. Test results have shown that the cumulative displacements measured along the length of the geogrid during cyclic loading increased significantly with the pre-cyclic pullout load level and the load amplitude. In contrast, the cumulative cyclic displacements were found to decrease with increasing frequency and soil density. In medium dense soil conditions, the geogrid post-cyclic pullout resistance decreased by up to 20%, with respect to the value obtained in the comparable monotonic test. However, for dense soil, the effect of cyclic loading on the peak pullout forces recorded during the tests was almost negligible.

KEYWORDS: Geosynthetics, Pullout tests, Cyclic loading, HDPE uniaxial geogrid, Granite residual soil, Frequency, Amplitude

1 INTRODUCTION

In recent decades, the use of geosynthetics as reinforcing elements in permanent earth structures, such as road and railway embankments, steep slopes, bridge abutments and retaining walls to improve the mechanical behaviour of soil has become a well-established technology worldwide. In fact, several advantages such as the relatively low cost, reduced construction time, ductility and flexibility, possibility to use lower quality locally available soils and adequate performance of geosynthetic-reinforced soil structures constructed even in seismic areas have led to their increasing use over their conventional counterparts. The geosynthetic tensile strength and the interaction characteristics at soil-reinforcement interfaces are crucial parameters for the internal stability analysis and safe design of such structures (Jewell 1996; Ferreira *et al.* 2015b; Ferreira *et al.* 2016a; Vieira and Pereira 2016). In particular, a condition for verification of internal stability is that the tensile force acting on the geosynthetic reinforcement should not exceed the pullout resistance in the anchorage zone (i.e. beyond the potential failure surface). Accordingly, the pullout capacity of geosynthetic reinforcement layers in the anchorage zone of geosynthetic-reinforced soil walls and slopes is required by design codes for stability analysis (BSI 1995; NCMA 1997; Canadian Geotechnical Society 2006; FHWA 2009; AASHTO 2017). Furthermore, internal stability checks often involve evaluation of serviceability requirements, such as maximum admissible lateral movements of supported structures.

In addition to static sustained loads (e.g. self-weight and eventual external dead loads), geosynthetic-reinforced soil systems are often subjected to repeated or cyclic loads both during construction and service life, which may arise from compaction, road and railway traffic (such as reinforced embankments and retaining walls in transportation infrastructure projects), wave loading (e.g. coastal structures) and earthquakes (when these structures are built in seismically active zones). Despite the generally high performance of these structures, some case histories of geosynthetic-reinforced retaining walls and bridge abutments have reported relatively large deformations resulting from traffic or seismic loading, which has occasionally been attributed to the use of low quality backfill materials and/or lack of seismic design consideration (Ling *et al.* 2001; Lee and Wu 2004). Given that soil-geosynthetic interface response under cyclic loading may significantly diverge from that under static loading, a thorough understanding of soil-reinforcement interaction under both monotonic and cyclic loading conditions is essential for the development of reliable design methodologies for geosynthetic-reinforced soil structures. However, while the static shear properties of soil-geosynthetic interfaces have been investigated by numerous researchers over the past decades (Farrag *et al.* 1993; Nakamura *et al.* 1999; Palmeira 2004; Moraci and Gioffrè 2006; Moraci and Recalcati 2006; Huang and Bathurst 2009; Liu *et al.* 2009; Palmeira 2009; Sieira *et al.* 2009; Ferreira *et al.* 2013; Esmaili *et al.* 2014; Ferreira *et al.* 2014; Lopes *et al.* 2014; Ferreira *et al.* 2015a; Ferreira *et al.* 2015b; Hatami and Esmaili 2015; Ferreira *et al.* 2016c; Ferreira *et al.* 2016d; Roodi *et al.* 2018; Mirzaalimohammadi *et al.* 2019; Morsy *et al.* 2019), very limited research has been undertaken to characterise the performance of soil-geosynthetic interfaces under cyclic loading (Raju and Fannin 1997, 1998; Moraci and Cardile 2009, 2012; Vieira *et al.* 2013; Ferreira *et al.* 2016b; Razzazan *et al.* 2018; Cardile *et al.* 2019; Razzazan *et al.* 2019). The complexity and number of factors that can influence soil-geosynthetic interaction under repeated or cyclic loads and the lack of systematic studies on the topic justify why the dynamic behaviour of geosynthetic-reinforced soil structures is still not well understood.

Various test methods including the direct shear test, triaxial test, inclined plane test, in-soil tensile test and pullout test have been used by different researchers to quantify soil-geosynthetic interaction. Of these, pullout and direct shear tests are the most commonly used.

This manuscript is the accepted version of the paper:

HDPE geogrid-residual soil interaction under monotonic and cyclic pullout loading, Geosynthetics International, Vol. 27, Issue 1, pp. 79-96, https://doi.org/10.1680/jgein.19.00057

While the direct shear test is a valuable test method for the assessment of soil-geosynthetic interaction when sliding of the soil mass on the reinforcement surface is likely to occur, the pullout test is better suited to describe the interaction between the soil and the geosynthetic in the anchorage zone (Palmeira 2009; Lopes 2012). In general, a pullout test is carried out by applying an axial load to an instrumented geosynthetic specimen embedded in a soil mass under a given normal stress value. The test yields the pullout resistance of the geosynthetic as well as the displacements and strains throughout the reinforcement length. While monotonic pullout testing allows interaction properties to be determined for situations where displacements are slow and steady, cyclic pullout testing can more accurately characterise the dynamic interaction between geosynthetics and the surrounding soil.

Raju and Fannin (1998) carried out a series of monotonic and cyclic pullout tests on various geosynthetics (i.e. geogrids and geomembranes) embedded in a uniformly graded sand to evaluate the influence of the confining stress, specimen properties and cyclic loading frequency on the mobilised pullout resistance and deformative behaviour of the specimens. The authors found that the pullout response is dependent upon the geogrid type. Two different geogrids experienced degradation of pullout resistance due to cyclic loading, whereas the third one yield a pullout resistance that was equal to or greater than that in the corresponding monotonic test. The tests also suggested that the geogrid pullout resistance is insensitive to the loading frequency.

Cuelho and Perkins (2005) evaluated the resilient shear modulus of geosynthetic-aggregate interfaces through a series of short-strip cyclic pullout tests. To minimise strains along the length of the geosynthetics, sample lengths were limited to 80 mm. The results showed that the interface shear modulus is stress dependent, increases with normal stress and decreases with increasing shear stress. The authors recognised that additional research is needed to identify the main factors affecting the results of cyclic pullout tests and establish specific test protocols with regard to specimen dimensions, instrumentation and loading conditions.

The pullout behaviour of uniaxial geogrids in loose and dense uniform silica sand and subjected to monotonic and cyclic pullout forces was investigated by Nayeri and Fakharian (2009). In this study, the post-cyclic pullout resistance of the reinforcement ranged from minus

10% (under higher normal pressures) to plus 20% (under lower normal pressures) with respect to the corresponding monotonic values. Unexpectedly, the accumulated displacements during cyclic loading in dense soil condition exceeded those recorded in loose soil condition. The increase of vertical pressure led to a reduction of the measured nodal displacements (due to restrained sliding of the reinforcement), but the deformations along the length of the geogrid were found to increase.

Moraci and Cardile (2009, 2012) studied the effect of a cyclic tensile load on the pullout resistance and deformative behaviour of geogrids embedded in a compacted uniform medium sand. By comparing the data obtained under monotonic and cyclic loading conditions, the authors concluded that cyclic loading may lead to a significant reduction of the reinforcement pullout resistance (by up to 30%). The loading amplitude and the normal pressure acting at the reinforcement level were found to be important factors with respect to the pullout resistance and deformation behaviour of the studied geogrids. In contrast, the influence of frequency was almost negligible.

To investigate the factors controlling soil-geogrid interface behaviour under cyclic loading, Abdel-Rahman and Ibbrahim (2011) carried out a laboratory study involving monotonic and cyclic pullout tests on geogrids embedded in a medium to fine siliceous sand. The authors concluded that the horizontal displacements of the geogrids under cyclic loading increase with the number of cycles until full slippage. Furthermore, geogrids of higher stiffness were found to withstand a larger number of load cycles than geogrids of lower stiffness before experiencing pullout failure. As expected, the incremental geogrid displacements per load cycle were higher at lower normal stress levels.

To better understand the effect of cyclic loading on the pullout resistance of a uniaxial geogrid embedded in uniformly graded sand at low density, Koshy and Unnikrishnan (2016) carried out a series of pullout tests under very low normal stresses (from 3 to 5 kPa). The authors concluded that the normal stress and the cyclic loading amplitude may affect the number of cycles leading to pullout failure. The post-cyclic monotonic tests revealed an important degradation of the geogrid pullout resistance due to cyclic loading and this effect became more pronounced as the number of cycles was increased.

Recently, Cardile *et al.* (2019) evaluated the pullout behaviour of a uniaxial geogrid embedded in a uniform medium sand under cyclic loading conditions. The authors found that the increase in cyclic loading amplitude adversely affects the stability of the sand-geogrid interface, whereas the increase in normal stress plays a stabilising role. They further pointed out that the peak pullout resistance of the geogrid under cyclic conditions may significantly decrease (by up to 28%) in comparison with the corresponding monotonic values.

From the above summary, it becomes apparent that the limited number of studies reported in the literature addressing the pullout behaviour of geosynthetics under cyclic loading conditions have generally been conducted using uniformly graded sands. In this current study, the load-strain-displacement behaviour of a uniaxial geogrid embedded in a locally available well-graded granite residual soil is examined through a series of large-scale pullout tests under monotonic and cyclic loading. The influence of various parameters, such as the frequency and amplitude of the cyclic pullout load, number of cycles, pre-cyclic pullout load level and soil placement density on the pullout response of the reinforcement is evaluated and discussed. A comparison is made between the maximum pullout forces mobilised during monotonic and multistage tests performed under identical physical conditions, enabling the potential degradation of the geogrid pullout resistance upon cyclic loading to be analysed in detail.

2 MATERIALS AND METHODS

2.1 Pullout test apparatus

The large-scale pullout test apparatus used in this experimental research comprises a pullout box consisting of a modular structure with internal dimensions of 1.53 m long, 1.00 m wide and 0.80 m deep. To minimise the frictional effects of the front wall boundary, the apparatus is equipped with a steel sleeve (0.20 m long and 0.48 m wide). To reduce the top boundary-soil friction and to achieve more uniform distribution of normal stresses, a 0.025 m thick smooth neoprene slab is placed between the soil and the loading plate. The clamping system is inserted into the test box through the sleeve, which minimises the initial unconfined length of the specimens. The normal stress on the top of the soil is applied through a wooden plate, which is loaded by ten small hydraulic jacks. A load cell is placed between one of the hydraulic jacks and the loading plate to control the magnitude of the applied normal pressure. The pullout force is transmitted to the geosynthetic specimen by means of a hydraulic system and is measured by a load cell. The geosynthetic frontal displacement is recorded by a linear potentiometer and the internal displacements are monitored using inextensible wires attached to the geosynthetic specimen at selected measurements points, with the opposite ends connected to linear potentiometers placed outside the pullout box. The tests are driven by a closed-loop servo-hydraulic control system, with capability for accurately measuring, controlling and recording the loads and displacements. The photographic views of the pullout test apparatus and an instrumented geogrid specimen are presented in Figure A.1 of the Supplemental Material to this paper (Appendix A). Further details on the equipment can be found in previous publications (Lopes and Ladeira 1996a, 1996b; Lopes and Silvano 2010; Ferreira *et al.* 2016d).

2.2 Materials

The soil used in this study was a locally available granite residual soil, which is typically found in the northern region of Portugal and widely used as backfill material for reinforced soil construction. According to the Unified Soil Classification System (ASTM D 2487-11:2011), this soil may be classified as SW-SM (well-graded sand with silt and gravel). The main physical and mechanical properties of the soil are presented in Table 1. The corresponding particle size distribution curve is shown in Figure A.2 of the Supplemental Material (Appendix A).

The reinforcement tested was a uniaxial extruded geogrid manufactured from high-density polyethylene (HDPE). Table 2 lists the main physical and mechanical properties of this geogrid. The in-isolation tensile strength was evaluated by tensile tests performed according to EN ISO 10319:2008 (CEN 2008). The obtained load-strain curves for five geogrid specimens tested under repeatability conditions can be found in Figure A.3 of the Supplemental Material (Appendix A).

HDPE geogrid-residual soil interaction under monotonic and cyclic pullout loading, Geosynthetics International, Vol. 27, Issue 1, pp. 79-96, https://doi.org/10.1680/jgein.19.00057

2.3 Test procedures

For each test, the soil was poured into the pullout box from a constant height of 0.50 m and compacted in four layers using an electric vibratory hammer. The geogrid specimen with initial dimensions of 0.33 m wide and 1.00 m long was clamped and laid over the first two layers of compacted soil. To monitor the displacements along the geogrid, four inextensible wires with one end attached to the specimen and the other end connected to linear potentiometers at the back of the pullout box were used. The remaining soil was then placed and compacted until a total height of soil of 0.60 m was reached. A neoprene sheet and a wooden plate were positioned on the top soil layer and the normal pressure was applied.

The monotonic pullout tests were carried out under both displacement- and load-controlled conditions, for comparison purposes. Following the European Standard EN 13738:2004 (CEN 2004), a constant displacement rate of 2 mm/min was imposed in the displacement-controlled tests. According to this standard, pullout tests may also be conducted using constant stress loading methods, such as the controlled stress rate method, where the pullout force is applied to the geosynthetic under a uniform loading rate not exceeding 2 kN/m/min until pullout or failure of the geosynthetic occurs. Accordingly, the load-controlled tests were performed at a constant load increment rate of 0.2 kN/min (corresponding to approximately 0.7kN/m/min).

The multistage pullout tests consisted of three successive phases carried out under load-controlled mode. Preliminary testing showed that, due to limitations of the test apparatus, the transitions between displacement- and load-controlled phases were not sufficiently smooth. Hence, all three phases of the multistage tests were performed under load-controlled conditions. In the first phase, a constant load increment rate of 0.2 kN/min was imposed. When the pullout force reached a targeted value (referred to in this paper as the pullout load level at the start of cyclic loading, P_S), specified as a function of the pullout resistance (P_R) obtained from load-controlled monotonic tests, a sinusoidal cyclic tensile load of constant frequency (f) and amplitude (A_F) was applied (starting with a loading path) for a given number of cycles (n). In the third phase, the test proceeded again under constant load increment rate (0.2 kN/min), until the pullout or tensile failure of the reinforcement was achieved. In order to determine whether or not the geogrid pullout resistance was affected by the cyclic loading histories, a comparison was made between the maximum pullout forces recorded in these tests (during the third phase) and that obtained from the load-controlled monotonic test performed under otherwise identical test conditions.

During the tests, the pullout force, frontal displacement, displacements over the length of the geogrid and applied normal stress were continuously monitored. To ensure accuracy of test results, all of the measurement devices were previously calibrated.

2.4 Test programme

Table 3 summarises the test conditions analysed in the present study. The geogrid pullout behaviour under monotonic loading was investigated by displacement- and load-controlled tests (tests T1 to T4) involving two different soil placement densities ($I_D = 50\%$ and $I_D = 85\%$, corresponding to γ_d = 15.3 kN/m and γ_d = 17.3 kN/m, respectively). The same soil density conditions were also adopted in the multistage tests (tests T5 to T20) for comparison purposes. Although geosynthetic-reinforced soil structures are typically constructed using densely compacted backfill materials to ensure adequate performance throughout their design life, the use of the lower density in this study ($I_D = 50\%$) aimed at enabling the assessment of the effect of soil placement density on the pullout response of the reinforcement. To investigate the influence of the static pullout load level at which the cyclic loading phase begins (P_S), different P_S/P_R ratios (where P_R is the maximum pullout force obtained under monotonic loading) were selected (P_S/P_R = 0.25, 0.50 and 0.65). The effects of the loading frequency (f) and amplitude (A_F) were examined by imposing sinusoidal waves with frequencies of 0.01, 0.1 and 1 Hz and normalised amplitudes (A_F/P_R) of 0.15, 0.40 and 0.60. The number of loading cycles (n) ranged from 40 to 120. In order to mimic low depths, where the pullout failure mechanism is most likely to occur in reinforced soil walls and slopes, a relatively low normal stress (σ_n = 25 kPa) was applied in all of the tests.

3 RESULTS AND DISCUSSION

3.1 Results from monotonic tests

Figures 1a and 1b compare the results from monotonic tests T1 and T2 conducted under displacement- and load-controlled mode, respectively, and using medium dense soil (I_D = 50%). The pattern of the pullout force-frontal displacement curves can be characterised by four different phases: an initial phase with a linear force-displacement relationship, followed by a nonlinear transition phase up to the maximum pullout force, after which the pullout force tends to decrease with further displacement of the clamped geogrid end, and finally a steady state is reached, where the pullout resistance is nearly constant (Figure 1a). It can be observed that the maximum pullout resistance attained in the load-controlled test exceeded that recorded under displacement-controlled conditions. The displacements recorded by the potentiometers over the length of the geogrid at maximum pullout force are given in Figure 1b. This figure reveals a non-linear stress distribution along the reinforcement length, which is typically observed in geosynthetic pullout tests due to the extensible nature of geosynthetics and the development of progressive failure mechanisms at the interface. Figure 1b also shows that the displacements measured along the reinforcement in the load- and displacement-controlled tests were rather similar, which is related to the fact that the maximum pullout force was achieved at a similar frontal displacement in both tests. The relatively high displacement value at the rear end of the specimen (≈36 mm) at maximum pullout force clearly indicates that the failure was caused by sliding of the geogrid along the interface (i.e. the geogrid specimen was pulled out from the soil).

The variations of pullout force with frontal displacement and the distribution of displacements along the geogrid at maximum pullout force obtained from displacement- and load-controlled tests (T3 and T4) involving dense soil (I_D = 85%) are presented in Figures 1c and 1d, respectively. The pullout force-displacement curves from both tests are qualitatively similar, exhibiting a stiff interface behaviour with a peak pullout force that is substantially higher than that recorded in the tests involving medium dense soil, followed by a sudden drop of the pullout force beyond the peak value. Similar to what was observed for I_D = 50%, a greater peak pullout resistance was reached in the load-controlled test (Figure 1c). It is noteworthy that in these tests the failure was caused by the reinforcement rupture in its first confined section (close to the front end), which implies that the pullout resistance was higher than the geogrid tensile strength under these confinement conditions. Interestingly, the in-soil tensile strength of the geogrid was considerably lower than the tensile strength obtained from in-isolation tests performed according to EN ISO 10319:2008 (Table 2). As shown in Figure 1d, high strains were generated along the front segments of the reinforcement and neither relevant slip nor large deformation were observed in the rear sections. This indicates that the greatest portion of the applied load was mobilised along the front part of the geogrid and only a small fraction of the load was transferred to the sections located towards its free end, which induced the tensile failure of the specimen. The high level of tension mobilised against the first confined transverse bar of the geogrid associated with the development of the passive resistance mechanism is likely to have contributed to the premature failure of the reinforcement (i.e. at a tensile force that is significantly lower than the geogrid tensile strength under unconfined conditions). Slightly higher deformations were produced along the length of the geogrid in the load-controlled test, which is consistent with the greater peak pullout force (mobilised at larger frontal displacement) attained in this test.

The differences in the maximum pullout capacity obtained from the load- and displacement-controlled tests can be attributed to the distinct loading rates imposed in these tests. Because of the viscous, time-dependent response of polymeric geosynthetic reinforcements under tensile loads, the peak strength is sensitive to rate of loading and generally increases with the loading rate at failure (Lopes and Ladeira 1996a; Hirakawa *et al.* 2003; Kongkitkul *et al.* 2004; Vieira and Lopes 2013). While the displacement-controlled tests were performed under a uniform displacement rate (2 mm/min), in the load-controlled tests the displacement rate was adjusted by the automated closed-loop control system so as to keep a uniform rate of load application (0.2 kN/min) until the maximum pullout force was achieved. In other words, a decrease in the interface stiffness during a load-controlled test leads to an increase in the rate of displacement of the clamp, given that a higher displacement increment is required to mobilise the prescribed load increment within a specific period of time. When the pullout force approached the maximum value, the displacement rate experienced in the load-controlled tests exceeded that imposed in the displacement-controlled tests, which is believed to be on the basis of the higher peak pullout forces reached under load-controlled conditions.

Therefore, to ensure that the comparison of results from monotonic and multistage tests is not affected by loading rate effects, only the load-controlled monotonic tests (tests T2 and T4) are used in the following sections as benchmark to evaluate the influence of the cyclic loading histories on the pullout behaviour of the reinforcement.

3.2 Results from multistage tests

3.2.1 *Influence of the pullout load level at the start of cyclic loading (P_S)*

To investigate the effect of the pullout force acting on the reinforcement at the start of the cyclic loading stage, different values of P_S specified as a function of the maximum pullout resistance recorded during load-controlled monotonic tests (P_R) were considered (P_S/P_R = 0.25, 0.50 and 0.65). In these tests, the cyclic stage consisted of a series of 40 cycles at the frequency (f) of 0.01 Hz and amplitude (A_F) of 0.15 P_R. Figure 2a presents the evolution of the pullout force with frontal displacement from multistage test T6 conducted with medium dense soil (I_D = 50%) and for P_S/P_R = 0.50. The pullout force-displacement curves obtained for distinct P_S/P_R ratios (tests T5 to T7) are available as supplemental material (see Appendix B, Figure B.1). The monotonic curves are also included in these graphs for comparison purposes. Regardless of the P_S/P_R value, the cyclic loading histories induced a decrease in the maximum pullout resistance of the geogrid. Although the results do not reveal a consistent reduction of pullout capacity with increasing P_S/P_R ratio, the most relevant decrease (≈18%) was obtained for the highest P_S/P_R ratio (see Figure B.1c in the Supplemental Material). A photographic view of a representative geogrid specimen after pullout failure (test T6) is presented in the Supplemental Material (Appendix C, Figure C.1a).

The displacements recorded over the geogrid length just before the application of the load cycles (termed herein as pre-cyclic displacements) and those measured during cyclic loading with increasing number of cycles (n) for P_S/P_R = 0.50 are plotted in Figure 2b. The results for

This manuscript is the accepted version of the paper:

HDPE geogrid-residual soil interaction under monotonic and cyclic pullout loading, Geosynthetics International, Vol. 27, Issue 1, pp. 79-96, https://doi.org/10.1680/jgein.19.00057

different P_S/P_R ratios can be found in Figure B.2 of the Supplemental Material. It should be noted that the displacements from n = 1 to n = 40 were obtained at the maximum pullout force for a specific load cycle. Intuitively, increasing the pullout load level P_S would increase the pre-cyclic displacements throughout the geogrid length, since during the load transfer phase greater pullout forces are associated with larger frontal displacements, and hence higher displacements over the reinforcement length. In the case of P_S/P_R = 0.25 (see Figure B.2a in the Supplemental Material), the incremental displacements over the length of the specimen during cyclic loading were almost negligible, and only the first instrumented section (adjacent to the clamp) experienced appreciable deformation. However, for higher values of P_S/P_R, the displacements along the reinforcement increased continuously with increasing number of cycles, albeit at a progressively decreasing rate (e.g. Figure 2b). It can therefore be concluded that the pullout load level at which the cyclic loading starts has the potential to affect the incremental displacements induced by the load cycles along the geogrid length, as well as the mobilised length of the reinforcement.

The influence of P_S on the geogrid deformation behaviour during cyclic loading is further clarified in Figure 3, which shows the cumulative displacements at the front and rear ends of the specimens. It can be concluded that the cumulative displacements at either end of the reinforcement increased gradually with the P_S/P_R ratio. Moreover, for P_S/P_R = 0.25, the displacements nearly stabilised after about five cycles, whereas a distinct trend was observed for the highest P_S/P_R value, characterised by a significant accumulation of displacements until the end of the cyclic phase, thus revealing potentially unstable interface behaviour. This finding may be associated with the fact that, for higher values of P_S/P_R, the cyclic phase takes place at higher pullout load levels, where the nonlinear interface behaviour becomes more pronounced.

The effect of P_S/P_R on the geogrid pullout response was also investigated using dense soil (I_D = 85%) and the results for the P_S/P_R ratio of 0.50 are shown in Figure 4 (test T14). The data concerning all three P_S/P_R ratios (tests T13 to T15) are presented in Figures B.3 and B.4 of the Supplemental Material. Similar to the procedure used in the tests involving medium dense soil, the cyclic phase encompassed a series of 40 cycles at f = 0.01 Hz and A_F = 0.15 P_R (where P_R is the maximum pullout force recorded in the comparable monotonic test). It can be noted from

Figure 4a that no significant degradation of the peak pullout force occurred after cyclic loading. This may be attributed to the fact that, in both the monotonic and multistage tests carried out with dense soil, the failure occurred due to the reinforcement breakage within the first confined section (i.e. near the front end). A photographic view of a representative geogrid specimen after experiencing tensile failure (test T14) can be found in the Supplemental Material (Appendix C, Figure C.1b).

Figure 4b shows that the displacements recorded along the geogrid tended to increase throughout the load cycles. When the lowest value of P_S/P_R was applied (see Figure B.4a in the Supplemental Material), only the front section of the geogrid was mobilised during cyclic loading. However, with increasing P_S/P_R ratio, the adjacent sections of the geogrid started to contribute to the mobilised forces (e.g. Figure 4b). The results suggest that, only the geogrid length mobilised in the first stage of the test (monotonic loading) underwent additional deformations during the cyclic stage. In fact, at the rear section, which was practically not mobilised in the first stage of the tests, the incremental displacements during cyclic loading were almost negligible, irrespective of P_S/P_R. As shown in Figure 5a, the displacements at the clamped end of the reinforcement increased with the number of cycles, but the increment rate was clearly lower under $P_S/P_R = 0.25$, denoting more stable interface response. The magnitude of the cumulative frontal displacements was somewhat similar for $P_S/P_R = 0.50$ and 0.65, visibly exceeding that corresponding to the lowest P_S/P_R value. The displacements at the free end of the specimens were rather small in all of the tests (Figure 5b).

3.2.2 *Influence of the loading frequency (f)*

The effect of the loading frequency was evaluated through multistage tests involving medium dense (tests T6, T8 and T9) and dense soil (tests T14, T16 and T17). In these tests, when the pullout force reached the targeted valued ($P_S = 0.50\ P_R$), 40 load cycles were imposed at normalised loading amplitude, $A_F/P_R = 0.15$ and frequencies, $f = 0.01$, 0.1 and 1 Hz. Figure 6a presents the variation of the pullout force as a function of the frontal displacement from multistage test T8 performed using medium dense soil ($I_D = 50\%$) and for $f = 0.1$ Hz. The results obtained for the frequency range of 0.01-1 Hz can be found in Figure B.5 of the Supplemental Material. Regardless of the loading frequency, the geogrid pullout resistance measured in the post-cyclic phase of the multistage tests was lower than that in the comparable monotonic test (e.g. Figure 6a). Additionally, the degradation of pullout capacity after cyclic loading appears to increase with frequency. Indeed, the maximum reduction in the geogrid pullout resistance (≈20%) was obtained when the highest loading rate (f = 1 Hz) was adopted (see Figure B.5c in the Supplemental Material).

The displacement distributions along the reinforcement obtained during the cyclic phase of multistage test T8 (f = 0.1 Hz) are illustrated in Figure 6b, whereas the data associated with the different frequencies can be found in Figure B.6 of the Supplemental Material. The slight differences in the pre-cyclic displacements corresponding to the multistage tests T6, T8 and T9 are associated with the inevitable variability of test results. The results indicate that, for lower frequencies (f = 0.01 and 0.1 Hz), the incremental displacements along the geogrid were particularly relevant during the early loading cycles, with a noticeable reduction being observed after the initial five cycles (e.g. Figure 6b). However, in the test performed at the highest frequency (f = 1 Hz), this trend was less pronounced (see Figure B.6c in the Supplemental Material). Regarding the cumulative displacements at the geogrid front end during cyclic loading, Figure 7a shows that they increased progressively with the number of cycles and decreased with increasing frequency. The effect of frequency on the displacements recorded at the opposite geogrid end followed a similar trend, albeit less evident (Figure 7b). The reduction in the cumulative geogrid displacements associated with the frequency increase can be attributed to the intrinsic viscous properties and associated time-dependent deformation response of polymeric geosynthetic reinforcements when subjected to tensile loads (Bathurst and Cai 1994; Leshchinsky *et al.* 1997; Hirakawa *et al.* 2003; Kongkitkul *et al.* 2004; Nuntapanich *et al.* 2018; Perkins and Haselton 2019). Bathurst and Cai (1994) investigated the in-isolation cyclic load-strain behaviour of HDPE geogrid specimens and observed the effects of viscous-elastic creep, which were predominant at frequencies equal to or lower than 0.1 Hz. Kongkitkul *et al.* (2004) showed that the residual geosynthetic strain produced during a given cyclic loading history is mainly controlled by the total period of cyclic loading (i.e. is due essentially to the material viscous properties). The creep potential of a HDPE geogrid under cyclic tensile loads was also observed during the in-isolation tensile tests reported by Cardile *et al.* (2017), where the residual strain of the geogrid after a given number of cycles was found to increase with decreasing frequency owing to the considerably different loading times.

Figure 8 shows the geogrid pullout behaviour during multistage test T16 (f = 0.1 Hz) involving dense soil (I_D = 85%). Similar results obtained for the distinct frequencies are available in the Supplemental Material (Figures B.7 and B.8). As opposed to what was observed in the tests involving medium dense soil, the peak pullout force was not significantly affected by the cyclic loading, regardless of frequency (e.g. Figure 8a). Indeed, the differences in the maximum pullout forces appear to be insignificant and can be attributed to the production variability of the test specimens. This occurrence is possibly related to the fact that the failure was caused by insufficient tensile strength of the reinforcement (i.e. tensile failure), which seems to remain independent of previous cyclic loading histories. Notwithstanding, the cyclic loading induced an increase in the frontal displacement at which the maximum pullout force was reached (e.g. Figure 8a).

As shown in Figure 8b, the incremental deformations developed over the length of the geogrid specimen during cyclic loading tended to decrease with the number of cycles. Similar to the trend reported earlier for tests performed with medium dense soil, the accumulated displacements at the geogrid front end decreased considerably with increasing rate of loading (Figure 9a). On the other hand, the displacements produced near the free end of the specimens were almost negligible, regardless of frequency (Figure 9b).

3.2.3 *Influence of the loading amplitude (A_F)*

Figure 10a illustrates the pullout force-displacement curve from multistage test T10 conducted with medium dense soil (I_D = 50%) and for the normalised amplitude, A_F/P_R = 0.40. Additional results for distinct values of A_F/P_R (0.15, 0.40 and 0.60) are presented in Figure B.9 of the Supplemental Material (tests T8, T10 and T11). Also shown in these graphs is the companion pullout force-displacement curve obtained under monotonic loading conditions. It can be seen that, for lower normalised amplitudes (0.15 and 0.40), the post-cyclic pullout resistance of the geogrid was lower than that attained in the monotonic test (e.g. Figure 10a). The degradation of pullout resistance upon cyclic loading tended to be less pronounced as the loading amplitude was increased (see Figure B.9 in the Supplemental Material).

The profiles of the displacements developed over the geogrid length during the cyclic phase of multistage test T10 (A_F/P_R = 0.40) are presented in Figure 10b. The comparison of results for different amplitude ratios is shown in the Supplemental Material (Figure B.10). The data clearly indicate that the loading amplitude is a key factor affecting the geogrid deformations and the relative displacements at the soil-geogrid interface. In fact, the incremental displacements induced by the load cycles increased substantially with the amplitude (see Figure B.10 in the Supplemental Material). On the other hand, the increment rate of displacements tended to reduce with the number of cycles (e.g. Figure 10b). These observations are further supported by the graphs in Figure 11, which show that the cumulative cyclic displacements at the reinforcement front and rear ends are positively correlated with the amplitude. This finding is in agreement with the results of previous related studies (Raju 1995; Raju and Fannin 1998; Moraci and Cardile 2012; Cardile *et al.* 2019), where the increase in the cyclic loading amplitude was found to lead to significantly higher cumulative cyclic displacements of the geogrid reinforcement, thus adversely affecting soil-geogrid interface stability.

Figure 12 shows the geogrid pullout response during multistage test T18 (A_F/P_R = 0.40) involving dense soil. The results for A_F/P_R ratios ranging from 0.15 to 0.60 (tests T16, T18 and T19) can be found in the Supplemental Material (Figures B.11 and B.12). Figure 12a indicates that the cyclic loading history did not induce any degradation of the peak pullout force. A similar conclusion can be drawn from the analysis of the results for other amplitude values. However, the frontal displacement corresponding to the maximum pullout force tended to increase with the loading amplitude (see Figure B.11 in the Supplemental Material). As previously observed from the tests carried out with medium dense soil, the higher the normalised amplitude, the larger the incremental displacements along the reinforcement (see Figure B.12 in the Supplemental Material). Accordingly, the accumulated displacements at the geogrid ends caused by cyclic loading also increased progressively with the loading amplitude (Figure 13).

The cumulative displacements produced at the rear end (Figure 13b) were significantly lower than those in the presence of looser soil (Figure 11b). This is related to the additional confinement provided by the denser soil, which restrained the transfer of stresses throughout the length of the reinforcement. It should be pointed out that, for A_F/P_R = 0.60, the cumulative frontal displacements induced by cyclic loading under both dense and medium dense soil conditions (I_D = 50% and 85%) exceeded the limit displacement of 30 mm beyond which a geosynthetic-reinforced wall of medium height (up to 13 m) constructed with a granular fill material can be considered to be performing poorly or be potentially unstable (Allen and Bathurst 2002).

3.2.4 *Influence of the number of load cycles (n)*

As mentioned previously, the influence of the number of cycles (n) on the geogrid pullout behaviour was examined by varying the number of cycles (from 40 to 120) in multistage pullout tests performed with different soil placement densities (I_D = 50% and 85%).

Figures 14a and 14b depict the variations of the pullout force with the frontal displacement from multistage tests T10 and T12 performed with medium dense soil for n = 40 and n = 120, respectively. The increase in the number of cycles adversely affected the post-cyclic pullout capacity of the studied geogrid, comparatively with that obtained under monotonic loading conditions. This may be associated with the fact that, in the test involving 120 cycles, the geogrid frontal displacement at the end of the cyclic phase was close to the displacement leading to the interface failure in the monotonic test.

The geogrid internal displacements developed during the 120 load cycles (test T12) are plotted in Figure 14c, whereas Figure 14d presents the evolution of the cumulative displacements at the specimen front and rear ends. These results indicate that the increments of displacement along the reinforcement were particularly important during the initial twenty cycles. Thereafter, the displacements at both geogrid ends increased continuously and at a nearly constant rate until the end of the cyclic loading phase, showing unstable cyclic interface

This manuscript is the accepted version of the paper:

HDPE geogrid-residual soil interaction under monotonic and cyclic pullout loading, Geosynthetics International, Vol. 27, Issue 1, pp. 79-96, https://doi.org/10.1680/jgein.19.00057

behaviour. Nevertheless, the 120 load cycles applied in this test did not lead to pullout failure of the reinforcement.

Figures 15a and 15b show the effect of the number of cycles on the geogrid pullout response when embedded in soil compacted to I_D = 85% (tests T18 and T20). Unlike the behaviour observed when the geogrid was tested in medium dense soil, the increase in the number of cycles from 40 to 120 did not significantly influence the peak load capacity. However, the post-cyclic interface stiffness was found to increase with the number of cycles. This is possibly associated with the noticeable soil lifts generated at the front of the geogrid transverse bars during the cyclic phase in the test involving 120 load cycles (see Figure C.2 in the Supplemental Material), which promoted the mobilisation of the passive resistance against those bars during the post-cyclic (monotonic) stage.

The displacements recorded along the geogrid length and those accumulated at either end of the specimen when subjected to 120 load cycles (in dense soil) are presented in Figures 15c and 15d, respectively. It can be noted from Figure 15c that the displacements over the back half of the geogrid length were almost negligible. In the sections closer to the clamp, the incremental displacements were particularly relevant in the initial twenty cycles, with only minor increments being observed thereafter. As shown in Figure 15d, no displacements were detected at the free end of the reinforcement and the frontal displacements remained nearly constant after the first twenty cycles. These evidences reveal stable interface behaviour and highlight the importance of an effective compaction of the backfill material in the construction of geogrid-reinforced soil structures subjected to cyclic loadings.

3.3 Discussion

The assessment of in-service deformations of permanent geosynthetic-reinforced earth structures, such as retaining walls and bridge abutments is often necessary to ensure these deformations are kept within acceptable levels and satisfy serviceability requirements. Following the criteria presented by Allen and Bathurst (2002), a reference displacement value of 30 mm is considered herein as the maximum admissible cumulative displacement beyond which a geosynthetic-reinforced wall of medium height (<13 m) constructed with a granular backfill can be considered to exhibit marginal performance. Furthermore, a maximum reinforcement strain of 3% is taken as the threshold value that divides satisfactory from poor wall performance.

A summary of the pullout test data obtained in this study is given in Table 4. The results from monotonic tests T1 to T4, which were carried out at different soil densities and under load- and displacement-controlled conditions are presented in terms of the geogrid pullout resistance (P_R) and corresponding frontal displacement (u_{PR}). Regarding the multistage tests (T5 to T20), the table lists the accumulated (residual) displacements at the front end ($U_{f,ac}$) and rear end ($U_{r,ac}$) of the geogrid specimens measured at the end of the cyclic phase (i.e. when the cyclic pullout force returned to the value of P_S), the accumulated (residual) deformations at the front section of the geogrid (ε_f) and the average accumulated deformations along the length of the reinforcement due to cyclic loading (ε_m), the maximum pullout force mobilised in the tests (P_R) and the corresponding frontal displacement (u_{PR}), as well as the percent variations of P_R (ΔP_R) and u_{PR} (Δu_{PR}) with respect to the values recorded in the benchmark (load-controlled) monotonic test. Also included in this table is the interface failure mode observed in each test.

Table 4 shows that the cumulative frontal displacements of the geogrid ($U_{f,ac}$) were in the range of 3.9 - 55.4 mm for I_D = 50% and 3.5 - 33.7 mm for I_D = 85%, whereas the cumulative displacements measured at the rear end ($U_{r,ac}$) varied from 1.0 - 37.3 mm for I_D = 50% and ≈0.0 - 7.7 mm for I_D = 85%. In general, both the front and rear cumulative displacements of the geogrid were significantly larger for I_D = 50%, when compared with those for denser soil (I_D = 85%) under otherwise identical test conditions. This finding implies that soil placement density plays a major role in the serviceability performance of geosynthetic-reinforced structures subjected to cyclic or repeated loads. For the conditions investigated, the most influential cyclic loading parameters concerning the accumulation of displacements at the front and rear edges of the geogrid were the number of cycles (only for I_D = 50%), followed by the loading amplitude and the pullout force acting on the reinforcement at the start of the cyclic loading. Indeed, the increase in the number of cycles (for I_D = 50%), loading amplitude and pre-cyclic pullout load level led to remarkable increments in the total accumulated geogrid displacements. On the other hand, the accumulated frontal displacements decreased progressively with increasing

This manuscript is the accepted version of the paper:

HDPE geogrid-residual soil interaction under monotonic and cyclic pullout loading, Geosynthetics International, Vol. 27, Issue 1, pp. 79-96, https://doi.org/10.1680/jgein.19.00057

frequency. Comparing the measured cumulative geogrid displacements with the limit value of 30 mm fixed on the basis of the aforementioned performance criteria (Allen and Bathurst 2002), it becomes apparent that some of the cyclic loading histories imposed in this study led to residual displacements exceeding this reference value, particularly when the lower soil placement density was adopted (I_D = 50%). For I_D = 85%, however, only in test T19 carried out under the highest amplitude ratio (A_F/P_R = 0.60) was the accumulated frontal displacement higher (12%) than the threshold value.

It can also be observed from Table 4 that the accumulated deformations at the first instrumented section of the reinforcement varied from 0.5% to 4.3% for I_D = 50%, and from 0.7% to 4.8% for I_D = 85%, whereas the average accumulated deformations (along the specimen) ranged from 0.3% to 2.0% for I_D = 50%, and from 0.4% to 2.9% for I_D = 85%. Regardless of the test conditions, the deformations produced at the front section consistently exceeded the average deformations over the length of the geogrid. As expected, soil placement density influenced the deformation behaviour of the reinforcement during cyclic loading. The deformations at the front segment as well as the average deformations along the length of the geogrid tested in dense soil (for I_D = 85%) were generally higher than or equal to those measured in the presence of medium dense soil (I_D = 50%). From the comparison between the residual geogrid strains measured in the current study and the maximum admissible value defined above (3%), it is noted that the deformations at the front section of the reinforcement were occasionally higher than this limit value. In particular, relatively high strains in excess of 3% were generated when the highest values of pullout load level at the start of the cyclic stage (P_S/P_R = 0.65) and loading amplitude (A_F/P_R = 0.6) were imposed. Therefore, reducing the ratio of the static tensile force acting on the reinforcement to the reinforcement pullout capacity in the anchorage zone can be considered as a stabilising measure that will possibly restrain the development of geosynthetic strains in the event of cyclic loading. In practice, this can be accomplished, for instance, by increasing the length of the geosynthetic reinforcement layers.

Regarding the influence of cyclic loading on the maximum pullout resistance of the geogrid, Table 4 indicates that in the tests conducted with medium dense soil (I_D = 50%), in which a pullout mode of failure was detected, the degradation of pullout capacity due to cyclic loading reached as much as 20.4%. Despite the differences in backfill type and placement density, this reduction value is in reasonable agreement with the results reported by Cardile *et al.* (2019) for a HDPE geogrid tested in a uniform medium sand, in which the reduction in the geogrid peak pullout resistance due to the effects of cyclic loading reached about 16% under the same normal stress (25 kPa). Moreover, the degradation of pullout resistance measured in this study supports the design guidelines laid down in the Federal Highway Administration documents (FHWA 2009) for the seismic design of geosynthetic-reinforced soil structures, where the pullout resistance factor for dynamic loading is taken as 80% of that for static loading in the absence of dynamic pullout test data.

The values of the peak pullout force recorded in the post-cyclic phase of the multistage tests carried out using dense soil (I_D = 85%) were similar to the peak load capacity attained in the benchmark test (i.e. monotonic test conducted under load-controlled mode and identical physical conditions). The observed differences (≤ 4.5%) are likely associated with the production variability of the test specimens. When the surrounding soil is dense, the deformations along the geogrid length are restrained and high stresses are mobilised at the front part of the specimens, potentially leading to breakage of the material in tension (tensile failure). In such case, the application of cyclic loading does not seem to affect the maximum load that the reinforcement can withstand before experiencing internal rupture. In fact, regardless of the loading characteristics (pre-cyclic pullout load level, amplitude, frequency and number of cycles), the cyclic loadings applied in this study did not cause the degradation of the peak load capacity leading to tensile failure of the reinforcement. This finding extends the conclusions drawn earlier by Vieira and Lopes (2013) and Cardile *et al.* (2017) in terms of the negligible effect of cyclic loading histories on the post-cyclic tensile strength of different geosynthetics evaluated by in-isolation tensile tests, suggesting that this is also valid when geosynthetics are subjected to cyclic tensile loads under confinement conditions.

This manuscript is the accepted version of the paper:

HDPE geogrid-residual soil interaction under monotonic and cyclic pullout loading, Geosynthetics International, Vol. 27, Issue 1, pp. 79-96, https://doi.org/10.1680/jgein.19.00057

4 CONCLUSIONS

This study investigated the pullout behaviour of a HDPE uniaxial geogrid embedded in a granite residual soil (under two different placement densities) through a series of monotonic and multistage pullout tests. Special emphasis was placed on the influence of the cyclic loading characteristics (i.e. pre-cyclic pullout load level, frequency, amplitude and number of cycles) on the cyclic and post-cyclic pullout response of the reinforcement. Based on the obtained results, the following conclusions can be drawn.

- Soil density plays a major role in the geogrid pullout resistance under cyclic loading conditions. When the tests were conducted with medium dense soil (I_D = 50%), the application of cyclic loading led generally to the degradation of the geogrid pullout resistance (by up to 20%), comparatively with that obtained under monotonic loading. However, in the tests involving dense soil (I_D = 85%), in which the failure was caused by the reinforcement rupture, the load cycles did not significantly affect the peak load capacity recorded in the post-cyclic phase.
- The maximum pullout force mobilised in the tests carried out with dense soil (in which the geogrid specimens failed in tension) was considerably lower (≈ 23%) than the unconfined tensile strength of the reinforcement evaluated by in-isolation tensile tests.
- In the majority of tests, the displacements measured throughout the length of the geogrid during cyclic loading increased with the number of cycles at a progressively decreasing rate, denoting progressive stabilisation of the soil-geogrid interface response.
- In general, both the front and rear cumulative cyclic displacements of the geogrid were significantly larger for I_D = 50%, when compared with those measured in the presence of dense soil (I_D = 85%). The reverse trend was observed concerning the accumulated geogrid strains during cyclic loading, with the specimens tested in dense soil generally exhibiting more pronounced cumulative deformations.
- Regardless of soil density, the accumulated displacements at the front edge as well as along the length of the geogrid resulting from cyclic loading increased substantially with the loading amplitude and the static pullout force acting on the reinforcement at the start of the

cyclic loading phase. In contrast, the accumulated displacements decreased with increasing frequency.

- When the soil was tested in medium dense state, increasing the number of cycles by threefold led to higher cumulative frontal displacements, as well as to unstable interface behaviour, characterised by a fast rate of accumulation of displacements until the end of the cyclic phase. Conversely, for dense soil, the interface exhibited stable behaviour, with the incremental displacements being almost negligible after about 20 cycles.
- The deformations generated at the front section of the geogrid during cyclic loading consistently exceeded the average deformations along the length of the specimens.
- For the tested conditions, no interface failure was observed during the cyclic loading stage.

The results reported herein expand the knowledge on the performance of a HDPE uniaxial geogrid (widely used in the construction of reinforced soil structures) when subjected to cyclic and post-cyclic monotonic loads, considering the important role of soil density. Future studies involving different geosynthetics and normal stress values would be useful to provide further insight following the above conclusions. Since the pullout resistance of geosynthetic reinforcements (P_R) is a prominent parameter with regard to the internal stability of geosynthetic-reinforced soil systems, special care should be taken when defining the design value of P_R for structures subjected to dynamic loadings. When P_R is estimated based on monotonic testing, proper reduction factors should be considered to account for the effects of cyclic loading on the soil-geosynthetic interface strength for more reliable design and performance evaluation.

ACKNOWLEDGMENTS

This work was financially supported by the Research Project CDW_LongTerm, POCI-01-0145-FEDER-030452, funded by FEDER funds through COMPETE2020 - Programa Operacional Competitividade e Internacionalização (POCI) and by national funds (PIDDAC) through FCT/MCTES. The authors gratefully acknowledge the financial support from the Portuguese Foundation for Science and Technology (FCT) under Grant SFRH/BD/72886/2010.

This manuscript is the accepted version of the paper:

HDPE geogrid-residual soil interaction under monotonic and cyclic pullout loading, Geosynthetics International, Vol. 27, Issue 1, pp. 79-96, https://doi.org/10.1680/jgein.19.00057

NOTATION

Basic SI units are given in parentheses.

A_F – cyclic loading amplitude (N/m)

c – soil cohesion (Pa)

C_C – soil curvature coefficient (dimensionless)

C_U – soil uniformity coefficient (dimensionless)

D_{10} – diameter corresponding to 10% passing of soil (m)

D_{30} – diameter corresponding to 30% passing of soil (m)

D_{50} – diameter corresponding to 50% passing of soil (m)

e_{max} – maximum void ratio of soil (dimensionless)

e_{min} – minimum void ratio of soil (dimensionless)

f – cyclic loading frequency (Hz)

G – specific gravity of soil particles (dimensionless)

I_D – soil relative density (dimensionless)

n – number of loading cycles (dimensionless)

P_S – pullout load level at the start of the cyclic loading phase (N/m)

P_R – pullout resistance per unit width of reinforcement (N/m)

u_{PR} – frontal displacement at maximum pullout force (m)

$U_{f,ac}$ – accumulated displacement at the geogrid front end (m)

$U_{r,ac}$ – accumulated displacement at the geogrid rear end (m)

γ_d – soil dry unit weight (N/m^3)

ΔP_R – percent variation of P_R with respect to the value obtained under monotonic conditions (dimensionless)

Δu_{PR} – percent variation of u_{PR} with respect to the value obtained under monotonic conditions (dimensionless)

ε_f – accumulated deformation at the front section of the geogrid (dimensionless)

ε_m – average accumulated deformation over the length of the geogrid (dimensionless)

σ_n – normal stress (Pa)

ϕ – soil internal friction angle (degrees)

REFERENCES

AASHTO (2017). LRFD Bridge Design Specifications. 8th edition, American Association of State Highway and Transportation Officials, Washington, D.C., USA.

Abdel-Rahman, A. H. & Ibbrahim, M. A. (2011). Soil/geogrid behavior subjected to cyclic loading. *Geotechnical Special Publication*, 2011, pp. 3087-3096.

Allen, T. M. & Bathurst, R. J. (2002). Observed long-term performance of geosynthetic walls and implications for design. *Geosynthetics International,* **9**, No. 5-6, 567-606.

ASTM D 2487-11 (2011). Standard practice for classification of soils for engineering purposes (Unified Soil Classification System). ASTM International, West Conshohocken, Pennsylvania.

Bathurst, R. J. & Cai, Z. (1994). In-isolation cyclic load-extension behavior of two geogrids. *Geosynthetics International,* **1**, No. 1, 1-19.

BSI (1995). BS8006:1995. Code of practice for strengthened/reinforced soil and other fills. British Standards Institution, Milton Keynes, UK.

Canadian Geotechnical Society (2006). Canadian Foundation Engineering Manual, 4th ed., BiTech Publisher Ltd., Richmond, BC, Canada.

Cardile, G., Moraci, N. & Pisano, M. (2017). Tensile behaviour of an HDPE geogrid under cyclic loading: Experimental results and empirical modelling. *Geosynthetics International,* **24**, No. 1, 95-112.

Cardile, G., Pisano, M. & Moraci, N. (2019). The influence of a cyclic loading history on soil-geogrid interaction under pullout condition. *Geotextiles and Geomembranes (in press).*

CEN (2004). EN 13738:2004. Geotextiles and geotextile-related products - Determination of pullout resistance in soil. European Committee for Standardization, Brussels, Belgium.

CEN (2008). EN ISO 10319:2008. Wide-width tensile tests. European Committee for Standardization, Brussels, Belgium.

Cuelho, E. V. & Perkins, S. W. (2005). Resilient interface shear modulus from short-strip, cyclic pullout tests. *Geotechnical Special Publication*, 2005, pp. 2863-2873.

Esmaili, D., Hatami, K. & Miller, G. A. (2014). Influence of matric suction on geotextile reinforcement-marginal soil interface strength. *Geotextiles and Geomembranes,* **42**, No. 2, 139-153.

Farrag, K., Acar, Y. B. & Juran, I. (1993). Pull-out resistance of geogrid reinforcements. *Geotextiles and Geomembranes,* **12**, No. 2, 133-159.

Ferreira, F. B., Carlos, D. M., Vieira, C. S. & Lopes, M. L. (2015a). Soil-geogrid interaction in pullout conditions: influence of soil moisture content and density. *Proceedings of the XVI European Conference on Soil Mechanics and Geotechnical Engineering, ECSMGE 2015*, 2015, pp. 1421-1426.

Ferreira, F. B., Carneiro, J. R., Vieira, C. S. & Lopes, M. L. (2014). Soil-geogrid interaction in the inclined plane shear movement. *Proceedings of the 10th International Conference on Geosynthetics, ICG 2014*, 2014.

Ferreira, F. B., Topa Gomes, A., Vieira, C. S. & Lopes, M. L. (2016a). Reliability analysis of geosynthetic-reinforced steep slopes. *Geosynthetics International,* **23**, No. 4, 301-315.

Ferreira, F. B., Vieira, C. S. & Lopes, M. L. (2013). Analysis of soil-geosynthetic interfaces shear strength through direct shear tests. *Proceedings of the International Symposium on Design and Practice of Geosynthetic-Reinforced Soil Structures.*

Ferreira, F. B., Vieira, C. S. & Lopes, M. L. (2015b). Direct shear behaviour of residual soil–geosynthetic interfaces – influence of soil moisture content, soil density and geosynthetic type. *Geosynthetics International,* **22**, No. 3, 257-272.

Ferreira, F. B., Vieira, C. S. & Lopes, M. L. (2016b). Cyclic and post-cyclic shear behaviour of a granite residual soil-geogrid interface. *Procedia Engineering, Vol. 143, Advances in Transportation Geotechnics III*, 2016, pp. 379-386.

Ferreira, F. B., Vieira, C. S. & Lopes, M. L. (2016c). Soil-geosynthetic interface strength properties from inclined plane and direct shear tests - A comparative analysis. *Proceedings of GA 2016 - 6th Asian Regional Conference on Geosynthetics: Geosynthetics for Infrastructure Development*, 2016, pp. 925-937.

Ferreira, F. B., Vieira, C. S., Lopes, M. L. & Carlos, D. M. (2016d). Experimental investigation on the pullout behaviour of geosynthetics embedded in a granite residual soil. *European Journal of Environmental and Civil Engineering,* **20**, No. 9, 1147-1180.

FHWA (2009). Design of mechanically stabilized earth walls and reinforced soil slopes – Volume I, FHWA-NHI-10-024 (editors Berg, R.R., Christopher, B.R., Samtani, N.C.), Federal Highway Administration, Washington, D.C.

Hatami, K. & Esmaili, D. (2015). Unsaturated soil-woven geotextile interface strength properties from small-scale pullout and interface tests. *Geosynthetics International,* **22**, No. 2, 161-172.

Hirakawa, D., Kongkitkul, W., Tatsuoka, F. & Uchimura, T. (2003). Time-dependent stress-strain behaviour due to viscous properties of geogrid reinforcement. *Geosynthetics International,* **10**, No. 6, 176-199.

Huang, B. & Bathurst, R. J. (2009). Evaluation of soil-geogrid pullout models using a statistical approach. *Geotechnical Testing Journal,* **32**, No. 6, 489-504.

Jewell, R. A. (1996). *Soil Reinforcement with Geotextiles*. Construction Industry Research and Information Association and Thomas Telford Publishing, London, UK, 332 p.

Kongkitkul, W., Hirakawa, D., Tatsuoka, F. & Uchimura, T. (2004). Viscous deformation of geosynthetic reinforcement under cyclic loading conditions and its model simulation. *Geosynthetics International,* **11**, No. 2, 73-99.

Koshy, N. & Unnikrishnan, N. (2016). Geosynthetics under cyclic pullout and post-cyclic monotonic loading. *International Journal of Geosynthetics and Ground Engineering,* **2**, No. 2, 13.

Lee, K. Z. Z. & Wu, J. T. H. (2004). A synthesis of case histories on GRS bridge-supporting structures with flexible facing. *Geotextiles and Geomembranes,* **22**, No. 4, 181-204.

Leshchinsky, D., Dechasakulsom, M., Kaliakin, V. N. & Ling, H. I. (1997). Creep and stress relaxation of geogrids. *Geosynthetics International,* **4**, No. 5, 463-479.

Ling, H. I., Leshchinsky, D. & Chou, N. N. S. (2001). Post-earthquake investigation on several geosynthetic-reinforced soil retaining walls and slopes during the ji-ji earthquake of Taiwan. *Soil Dynamics and Earthquake Engineering,* **21**, No. 4, 297-313.

Liu, C. N., Ho, Y. H. & Huang, J. W. (2009). Large scale direct shear tests of soil/PET-yarn geogrid interfaces. *Geotextiles and Geomembranes,* **27**, No. 1, 19-30.

Lopes, M. L. (2012). Soil-geosynthetic interaction. In Handbook of Geosynthetic Engineering, Shukla, S. K., Editor, ICE Publishing, London, UK, pp. 45–66.

Lopes, M. L., Ferreira, F. B., Carneiro, J. R. & Vieira, C. S. (2014). Soil-geosynthetic inclined plane shear behavior: influence of soil moisture content and geosynthetic type. *International Journal of Geotechnical Engineering,* **8**, No. 3, 335-342.

Lopes, M. L. & Ladeira, M. (1996a). Influence of the confinement, soil density and displacement rate on soil-geogrid interaction. *Geotextiles and Geomembranes,* **14**, No. 10, 543-554.

Lopes, M. L. & Ladeira, M. (1996b). Role of specimen geometry, soil height and sleeve length on the pull-out behaviour of geogrids. *Geosynthetics International,* **3**, No. 6, 701-719.

Lopes, M. L. & Silvano, R. (2010). Soil/geotextile interface behaviour in direct shear and pullout movements. *Geotechnical and Geological Engineering,* **28**, No. 6, 791-804.

Mirzaalimohammadi, A., Ghazavi, M., Roustaei, M. & Lajevardi, S. H. (2019). Pullout response of strengthened geosynthetic interacting with fine sand. *Geotextiles and Geomembranes (in press).*

Moraci, N. & Cardile, G. (2009). Influence of cyclic tensile loading on pullout resistance of geogrids embedded in a compacted granular soil. *Geotextiles and Geomembranes,* **27**, No. 6, 475-487.

Moraci, N. & Cardile, G. (2012). Deformative behaviour of different geogrids embedded in a granular soil under monotonic and cyclic pullout loads. *Geotextiles and Geomembranes,* **32**, 104-110.

Moraci, N. & Gioffrè, D. (2006). A simple method to evaluate the pullout resistance of extruded geogrids embedded in a compacted granular soil. *Geotextiles and Geomembranes,* **24**, No. 2, 116-128.

Moraci, N. & Recalcati, P. (2006). Factors affecting the pullout behaviour of extruded geogrids embedded in a compacted granular soil. *Geotextiles and Geomembranes,* **24**, No. 4, 220-242.

Morsy, A. M., Zornberg, J. G., Han, J. & Leshchinsky, D. (2019). A new generation of soil-geosynthetic interaction experimentation. *Geotextiles and Geomembranes (in press).*

Nakamura, T., Mitachi, T. & Ikeura, I. (1999). Direct shear testing method as a means for estimating geogrid - Sand interface shear - Displacement behavior. *Soils and Foundations,* **39**, No. 4, 1-8.

This manuscript is the accepted version of the paper:

HDPE geogrid-residual soil interaction under monotonic and cyclic pullout loading, Geosynthetics International, Vol. 27, Issue 1, pp. 79-96, https://doi.org/10.1680/jgein.19.00057

Nayeri, A. & Fakharian, K. (2009). Study on pullout behavior of uniaxial HDPE geogrids under monotonic and cyclic loads. *International Journal of Civil Engineering,* **7**, No. 4, 211-223.

NCMA (1997). Design manual for segmental retaining walls (2nd ed.), National Concrete Masonry Association (ed. J. Collin), Herndon, VA, USA.

Nuntapanich, N., Kongkitkul, W., Tatsuoka, F. & Jongpradist, P. (2018). Prediction of creep behaviour from load relaxation behaviour of polymer geogrids. *Geosynthetics International,* **25**, No. 3, 334-349.

Palmeira, E. M. (2004). Bearing force mobilisation in pull-out tests on geogrids. *Geotextiles and Geomembranes,* **22**, No. 6, 481-509.

Palmeira, E. M. (2009). Soil-geosynthetic interaction: Modelling and analysis. *Geotextiles and Geomembranes,* **27**, No. 5, 368-390.

Perkins, S. W. & Haselton, H. N. (2019). Resilient response of geosynthetics from cyclic and sustained in-air tensile loading. *Geosynthetics International (in press).*

Raju, D. M. (1995). *Monotonic and cyclic pullout resistance of geosynthetics.* PhD Thesis, The University of British Columbia, Canada.

Raju, D. M. & Fannin, R. J. (1997). Monotonic and cyclic pull-out resistance of geogrids. *Geotechnique,* **47**, No. 2, 331-337.

Raju, D. M. & Fannin, R. J. (1998). Load-strain-displacement response of geosynthetics in monotonic and cyclic pullout. *Canadian Geotechnical Journal,* **35**, No. 2, 183-193.

Razzazan, S., Keshavarz, A. & Mosallanezhad, M. (2018). Pullout behavior of polymeric strip in compacted dry granular soil under cyclic tensile load conditions. *Journal of Rock Mechanics and Geotechnical Engineering,* **10**, No. 5, 968-976.

Razzazan, S., Keshavarz, A. & Mosallanezhad, M. (2019). Large-scale pullout testing and numerical evaluation of U-shape polymeric straps. *Geosynthetics International,* **26**, No. 3, 237-250.

Roodi, G. H., Morsy, A. M. & Zornberg, J. G. (2018). Soil–geosynthetic interface shear in different testing scales. *Transportation Research Record, DOI: 10.1177/0361198118758631 (in press).*

Sieira, A. C., Gerscovich, D. M. & Sayão, A. S. (2009). Displacement and load transfer mechanisms of geogrids under pullout condition. *Geotextiles and Geomembranes,* **27**, No. 4, 241-253.

Vieira, C. S. & Lopes, M. D. L. (2013). Effects of the loading rate and cyclic loading on the strength and deformation properties of a geosynthetic. *Construction and Building Materials,* **49**, 758-765.

Vieira, C. S., Lopes, M. L. & Caldeira, L. M. (2013). Sand-geotextile interface characterisation through monotonic and cyclic direct shear tests. *Geosynthetics International,* **20**, No. 1, 26-38.

Vieira, C. S. & Pereira, P. M. (2016). Interface shear properties of geosynthetics and construction and demolition waste from large-scale direct shear tests. *Geosynthetics International,* **23**, No. 1, 62-70.

This manuscript is the accepted version of the paper:

HDPE geogrid-residual soil interaction under monotonic and cyclic pullout loading, Geosynthetics International, Vol. 27, Issue 1, pp. 79-96, https://doi.org/10.1680/jgein.19.00057

LIST OF TABLES

This manuscript is the accepted version of the paper:

HDPE geogrid-residual soil interaction under monotonic and cyclic pullout loading, Geosynthetics International, Vol. 27, Issue 1, pp. 79-96, https://doi.org/10.1680/jgein.19.00057

LIST OF FIGURES

Figure 8. Pullout test results for f = 0.1 Hz (I_D = 85%, P_S/P_R = 0.50, A_F/P_R = 0.15, n = 40): (a) evolution of pullout force with frontal displacement; (b) displacements recorded along the geogrid during the cyclic loading phase.

Figure 9. Influence of frequency on the accumulated displacements at the geogrid ends during the cyclic loading phase (I_D = 85%, P_S/P_R = 0.50, A_F/P_R = 0.15, n = 40): (a) front end; (b) free end.

Figure 10. Pullout test results for A_F/P_R = 0.40 (I_D = 50%, P_S/P_R = 0.50, f = 0.1 Hz, n = 40): (a) evolution of pullout force with frontal displacement; (b) displacements recorded along the geogrid during the cyclic loading phase.

Figure 11. Influence of amplitude on the accumulated displacements at the geogrid ends during the cyclic loading phase (I_D = 50%, P_S/P_R = 0.50, f = 0.1 Hz, n = 40): (a) front end; (b) free end.

Figure 12. Pullout test results for A_F/P_R = 0.40 (I_D = 85%, P_S/P_R = 0.50, f = 0.1 Hz, n = 40): (a) evolution of pullout force with frontal displacement; (b) displacements recorded along the geogrid during the cyclic loading phase.

Figure 13. Influence of amplitude on the accumulated displacements at the geogrid ends during the cyclic loading phase (I_D = 85%, P_S/P_R = 0.50, f = 0.1 Hz, n = 40): (a) front end; (b) free end.

Figure 14. Influence of number of cycles on the pullout test results (I_D = 50%, P_S/P_R = 0.50, f = 0.1 Hz, A_F/P_R = 0.40): (a) evolution of pullout force with frontal displacement (n = 40); (b) evolution of pullout force with frontal displacement (n = 120); (c) displacements recorded along the geogrid during the cyclic phase (n = 120); (d) accumulated displacements at the geogrid ends (n = 120).

This manuscript is the accepted version of the paper:

HDPE geogrid-residual soil interaction under monotonic and cyclic pullout loading, Geosynthetics International, Vol. 27, Issue 1, pp. 79-96, https://doi.org/10.1680/jgein.19.00057

Figure 15. Influence of number of cycles on the pullout test results (I_D = 85%, P_S/P_R = 0.50, f = 0.1 Hz, A_F/P_R = 0.40): (a) evolution of pullout force with frontal displacement (n = 40); (b) evolution of pullout force with frontal displacement (n = 120); (c) displacements recorded along the geogrid during the cyclic phase (n = 120); (d) accumulated displacements at the geogrid ends (n = 120).

This manuscript is the accepted version of the paper:

HDPE geogrid-residual soil interaction under monotonic and cyclic pullout loading, Geosynthetics International, Vol. 27, Issue 1, pp. 79-96, https://doi.org/10.1680/jgein.19.00057

TABLES

This manuscript is the accepted version of the paper:

HDPE geogrid-residual soil interaction under monotonic and cyclic pullout loading, Geosynthetics International, Vol. 27, Issue 1, pp. 79-96, https://doi.org/10.1680/jgein.19.00057

Table 1. Soil physical and mechanical properties.

Property	Value	Unit
D_{10}	0.09	mm
D_{30}	0.35	mm
D_{50}	1.00	mm
C_U	16.90	-
C_C	1.00	-
G	2.73	-
e_{max}	0.998	-
e_{min}	0.476	-
ϕ (I_D = 50%)[1]	44.7	degree
c (I_D = 50%)[1]	7.8	kPa
ϕ (I_D = 85%)[1]	46.6	degree
c (I_D = 85%)[1]	29.5	kPa

[1] Obtained from large-scale direct shear tests (Ferreira *et al.* 2015b).

Table 2. Geogrid physical and mechanical properties.

Property	Value	Unit
Raw material	HDPE	-
Mass per unit area	450	g/m^2
Thickness of longitudinal ribs	1.1	mm
Thickness of transverse ribs	2.7	mm
Mean grid size	22×235	mm
Percent open area	59	%
Short term tensile strength[1]	68	kN/m
Elongation at maximum load[1]	11.0	%
Short term tensile strength[2]	52.2	kN/m
Elongation at maximum load[2]	12.4	%
Secant stiffness at 5% strain[2]	509.8	kN/m

[1] Provided by the manufacturer (machine direction).

[2] Obtained from tensile tests in the machine direction (according to EN ISO 10319:2008 (CEN 2008)).

Table 3. Test programme.

Test	Test procedure	I_D (%)	σ_n (kPa)	P_S/P_R	f (Hz)	A_F/P_R	n
T1[1]	Monotonic	50	25	-	-	-	-
T2	Monotonic	50	25	-	-	-	-
T3[1]	Monotonic	85	25	-	-	-	-
T4	Monotonic	85	25	-	-	-	-
T5	Multistage	50	25	0.25	0.01	0.15	40
T6	Multistage	50	25	0.50	0.01	0.15	40
T7	Multistage	50	25	0.65	0.01	0.15	40
T8	Multistage	50	25	0.50	0.1	0.15	40
T9	Multistage	50	25	0.50	1	0.15	40
T10	Multistage	50	25	0.50	0.1	0.40	40
T11	Multistage	50	25	0.50	0.1	0.60	40
T12	Multistage	50	25	0.50	0.1	0.40	120
T13	Multistage	85	25	0.25	0.01	0.15	40
T14	Multistage	85	25	0.50	0.01	0.15	40
T15	Multistage	85	25	0.65	0.01	0.15	40
T16	Multistage	85	25	0.50	0.1	0.15	40
T17	Multistage	85	25	0.50	1	0.15	40
T18	Multistage	85	25	0.50	0.1	0.40	40
T19	Multistage	85	25	0.50	0.1	0.60	40
T20	Multistage	85	25	0.50	0.1	0.40	120

[1] Carried out under displacement-controlled conditions.

This manuscript is the accepted version of the paper:

HDPE geogrid-residual soil interaction under monotonic and cyclic pullout loading, Geosynthetics International, Vol. 27, Issue 1, pp. 79-96, https://doi.org/10.1680/jgein.19.00057

Table 4. Summary of results.

Test	$U_{f,ac}$ (mm)	$U_{r,ac}$ (mm)	ε_f (%)	ε_m (%)	P_R (kN/m)	u_{PR} (mm)	ΔP_R (%)	Δu_{PR} (%)	Failure mode
T1	-	-	-	-	24.0	94.1	-	-	Pullout
T2	-	-	-	-	29.3	91.0	-	-	Pullout
T3	-	-	-	-	37.9	55.8	-	-	Tensile
T4	-	-	-	-	39.9	69.6	-	-	Tensile
T5	3.9	1.0	1.1	0.3	25.2	90.2	-13.9	-0.9	Pullout
T6	11.7	2.2	2.1	1.1	27.0	89.8	-7.8	-1.4	Pullout
T7	24.5	7.0	4.3	2.0	24.1	82.5	-17.7	-9.4	Pullout
T8	8.3	2.2	1.0	0.7	25.3	81.8	-13.6	-10.1	Pullout
T9	4.5	1.4	0.5	0.4	23.3	71.3	-20.4	-21.7	Pullout
T10	25.4	15.1	1.3	1.2	27.2	102.7	-7.1	12.8	Pullout
T11	38.4	22.6	3.3	1.8	28.5	93.6	-2.7	2.8	Pullout
T12	55.4	37.3	2.3	2.0	24.2	108.6	-17.3	19.3	Pullout
T13	3.5	0.0	1.3	0.4	40.4	66.8	1.2	-4.0	Tensile
T14	15.1	0.9	3.1	1.6	38.4	87.2	-3.8	25.4	Tensile
T15	16.6	0.4	4.8	1.8	39.7	67.7	-0.6	-2.7	Tensile
T16	6.4	0.2	2.0	0.7	41.0	82.5	2.7	18.6	Tensile
T17	4.0	0.5	0.7	0.4	38.3	80.4	-4.1	15.6	Tensile
T18	18.5	2.7	2.0	1.8	41.1	90.6	3.0	30.3	Tensile
T19	33.7	7.7	3.1	2.9	41.7	102.9	4.5	48.0	Tensile
T20	13.8	0.3	2.6	1.5	40.9	59.3	2.5	-14.7	Tensile

This manuscript is the accepted version of the paper:

HDPE geogrid-residual soil interaction under monotonic and cyclic pullout loading, Geosynthetics International, Vol. 27, Issue 1, pp. 79-96, https://doi.org/10.1680/jgein.19.00057

FIGURES

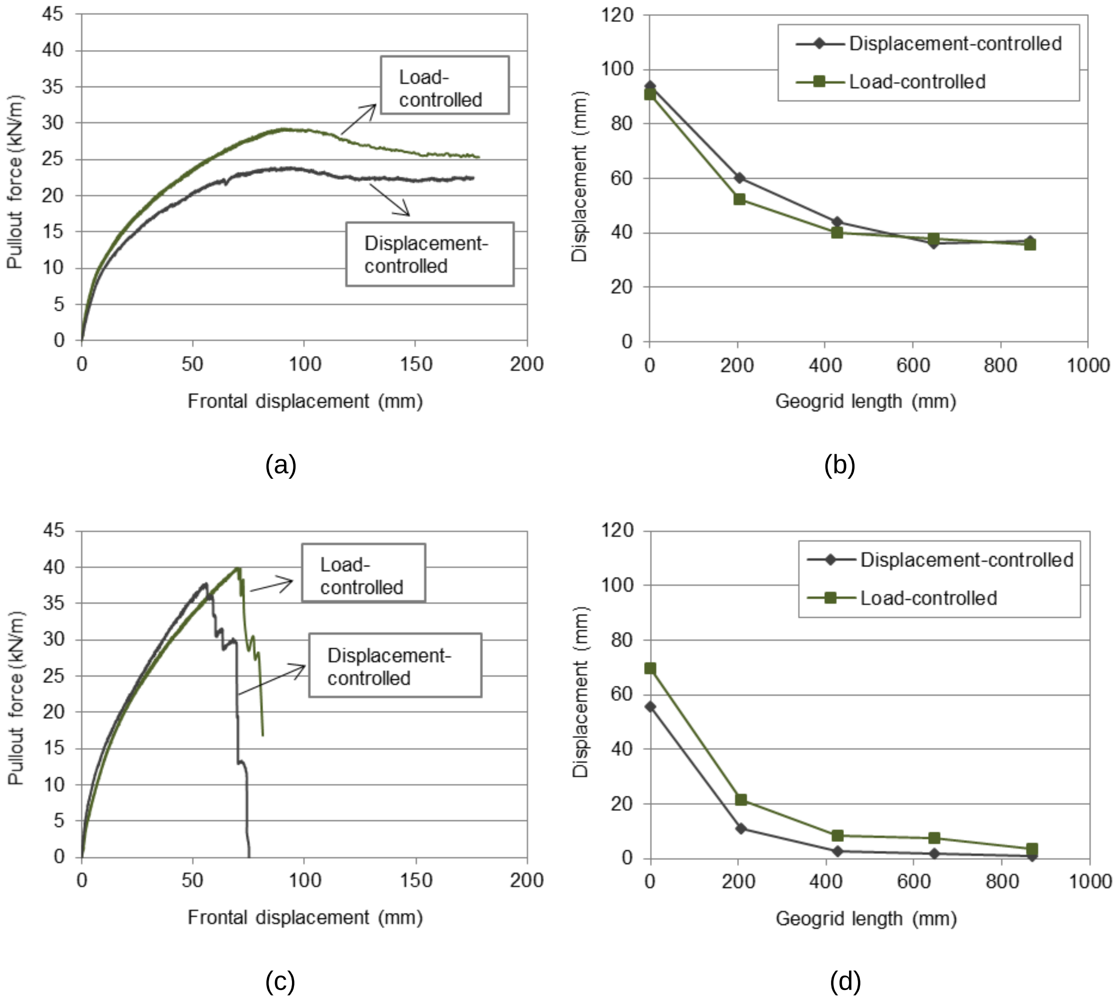

Figure 1. Pullout test results under monotonic loading (load- vs displacement-controlled conditions): (a) evolution of pullout force with frontal displacement (I_D = 50%); (b) displacements along the geogrid at maximum pullout force (I_D = 50%); (c) evolution of pullout force with frontal displacement (I_D = 85%); (d) displacements along the geogrid at maximum pullout force (I_D = 85%).

This manuscript is the accepted version of the paper:

HDPE geogrid-residual soil interaction under monotonic and cyclic pullout loading, Geosynthetics International, Vol. 27, Issue 1, pp. 79-96, https://doi.org/10.1680/jgein.19.00057

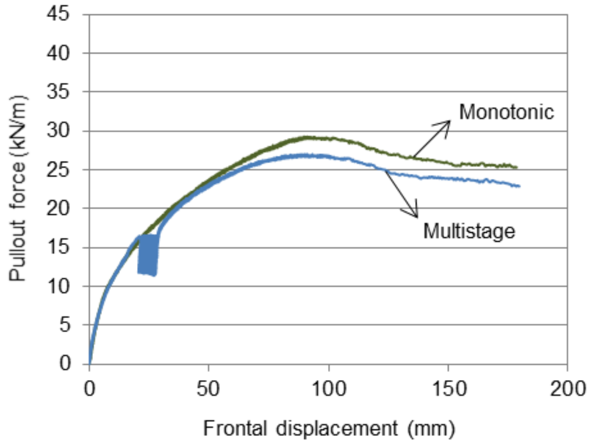

(a)

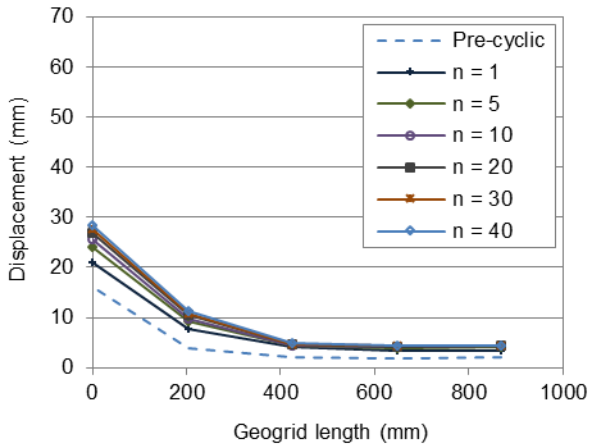

(b)

Figure 2. Pullout test results for $P_S/P_R = 0.50$ ($I_D = 50\%$, f = 0.01 Hz, $A_F/P_R = 0.15$, n = 40): (a) evolution of pullout force with frontal displacement; (b) displacements recorded along the geogrid during the cyclic loading phase.

This manuscript is the accepted version of the paper:

HDPE geogrid-residual soil interaction under monotonic and cyclic pullout loading, Geosynthetics International, Vol. 27, Issue 1, pp. 79-96, https://doi.org/10.1680/jgein.19.00057

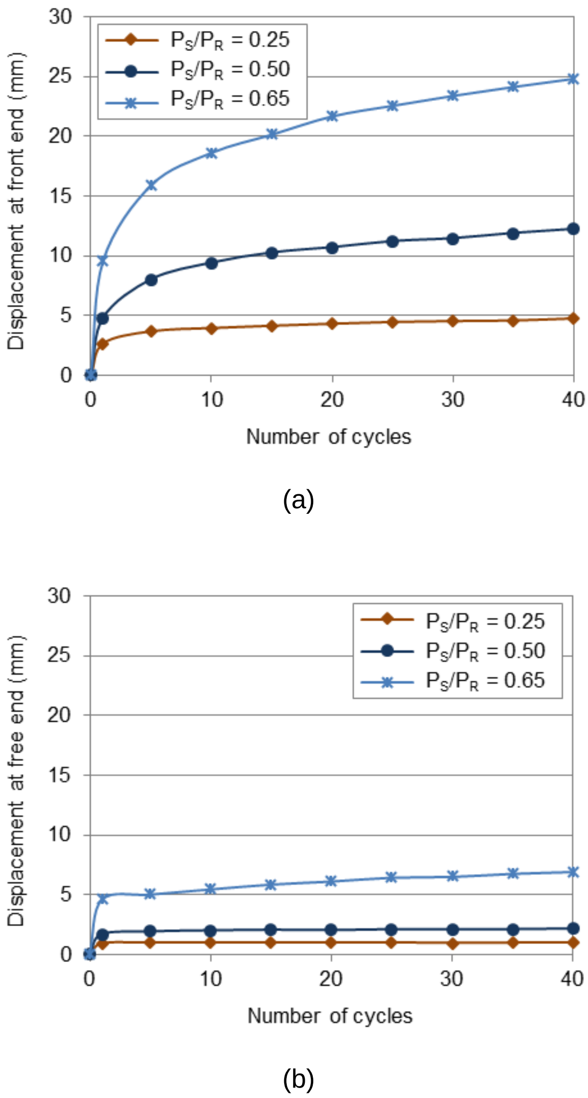

Figure 3. Influence of P_S on the accumulated displacements at the geogrid ends during the cyclic loading phase (I_D = 50%, f = 0.01 Hz, A_F/P_R = 0.15, n = 40): (a) front end; (b) free end.

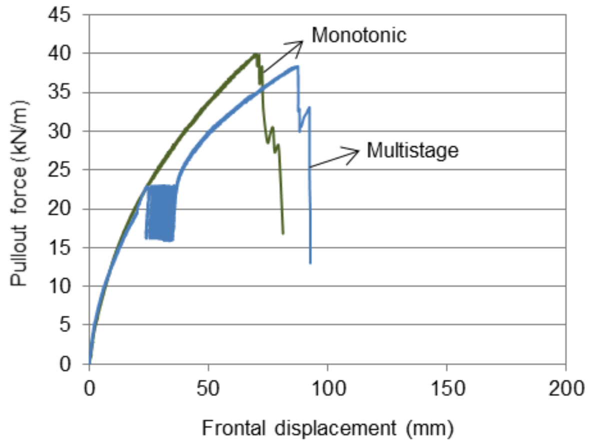

(a)

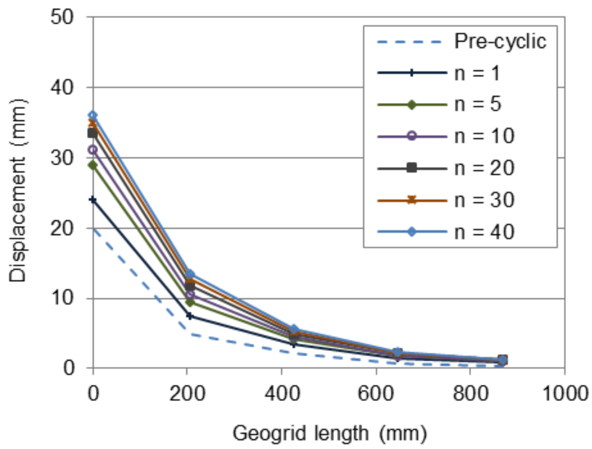

(b)

Figure 4. Pullout test results for P_S/P_R = 0.50 (I_D = 85%, f = 0.01 Hz, A_F/P_R = 0.15, n = 40): (a) evolution of pullout force with frontal displacement; (b) displacements recorded along the geogrid during the cyclic loading phase.

This manuscript is the accepted version of the paper:

HDPE geogrid-residual soil interaction under monotonic and cyclic pullout loading, Geosynthetics International, Vol. 27, Issue 1, pp. 79-96, https://doi.org/10.1680/jgein.19.00057

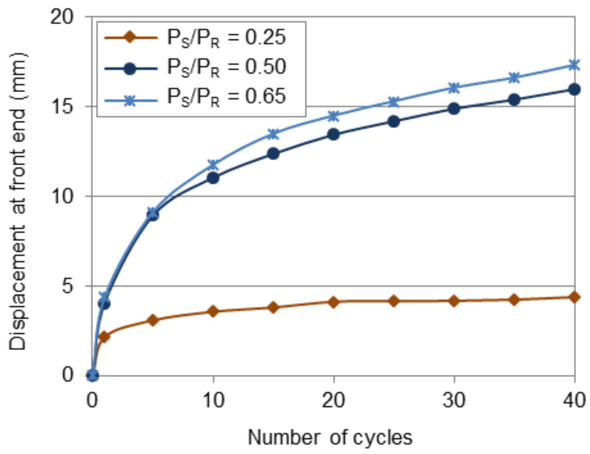

(a)

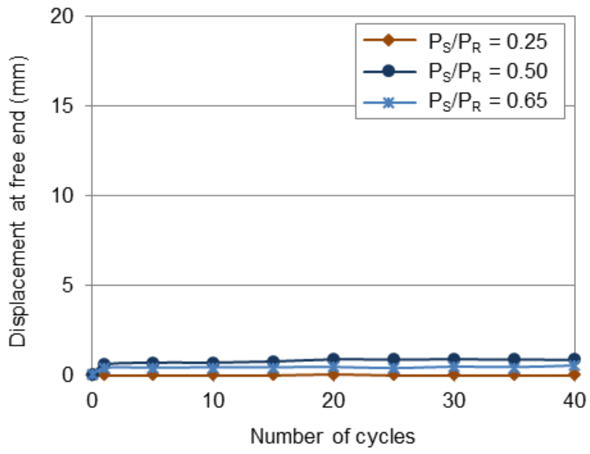

(b)

Figure 5. Influence of P_S on the accumulated displacements at the geogrid ends during the cyclic loading phase (I_D = 85%, f = 0.01 Hz, A_F/P_R = 0.15, n = 40): (a) front end; (b) free end.

This manuscript is the accepted version of the paper:

HDPE geogrid-residual soil interaction under monotonic and cyclic pullout loading, Geosynthetics International, Vol. 27, Issue 1, pp. 79-96, https://doi.org/10.1680/jgein.19.00057

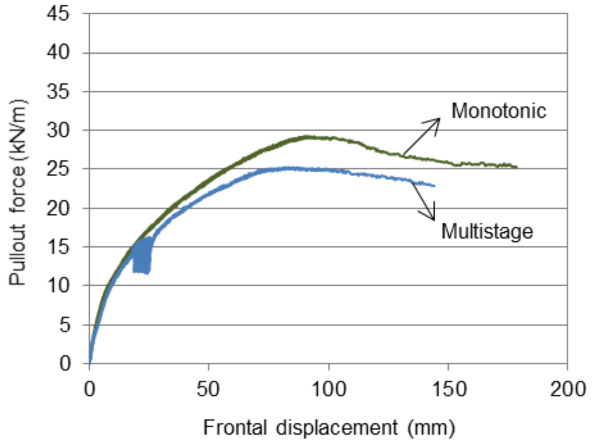

(a)

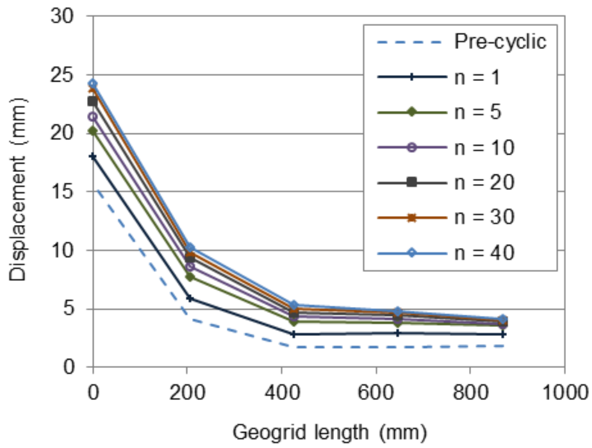

(b)

Figure 6. Pullout test results for f = 0.1 Hz (I_D = 50%, P_S/P_R = 0.50, A_F/P_R = 0.15, n = 40): (a) evolution of pullout force with frontal displacement; (b) displacements recorded along the geogrid during the cyclic loading phase.

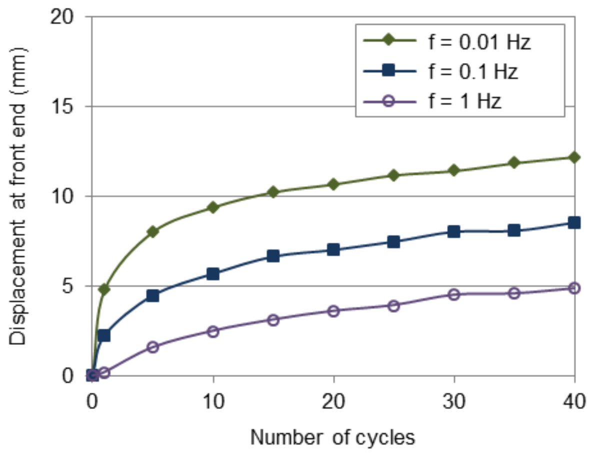

(a)

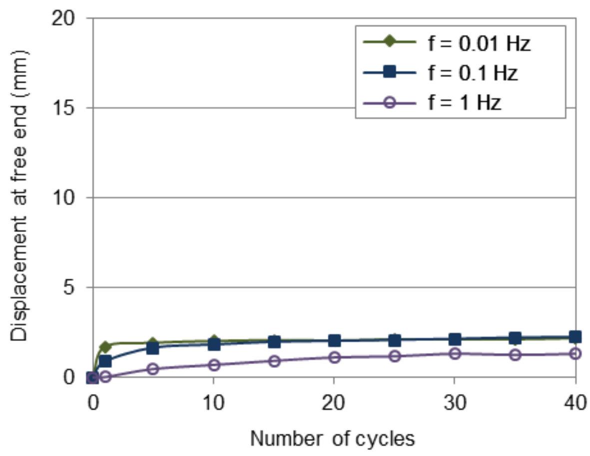

(b)

Figure 7. Influence of frequency on the accumulated displacements at the geogrid ends during the cyclic loading phase (I_D = 50%, P_S/P_R = 0.50, A_F/P_R = 0.15, n = 40): (a) front end; (b) free end.

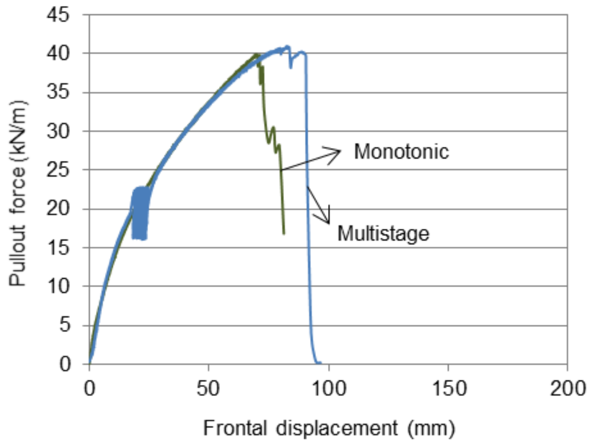

(a)

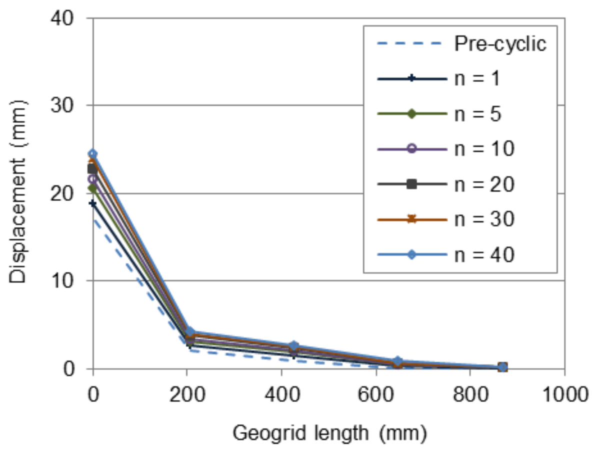

(b)

Figure 8. Pullout test results for f = 0.1 Hz (I_D = 85%, P_S/P_R = 0.50, A_F/P_R = 0.15, n = 40): (a) evolution of pullout force with frontal displacement; (b) displacements recorded along the geogrid during the cyclic loading phase.

This manuscript is the accepted version of the paper:

HDPE geogrid-residual soil interaction under monotonic and cyclic pullout loading, Geosynthetics International, Vol. 27, Issue 1, pp. 79-96, https://doi.org/10.1680/jgein.19.00057

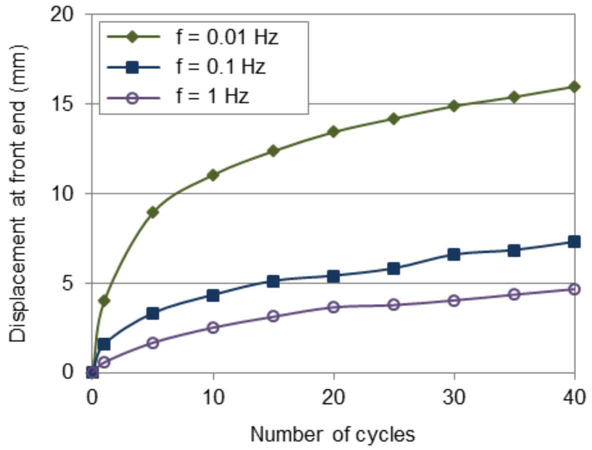

(a)

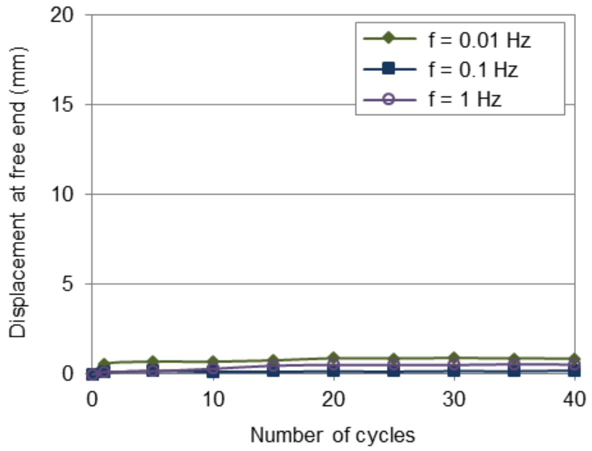

(b)

Figure 9. Influence of frequency on the accumulated displacements at the geogrid ends during the cyclic loading phase (I_D = 85%, P_S/P_R = 0.50, A_F/P_R = 0.15, n = 40): (a) front end; (b) free end.

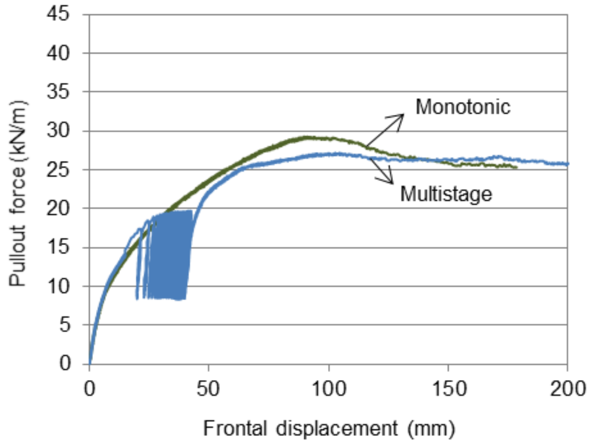

(a)

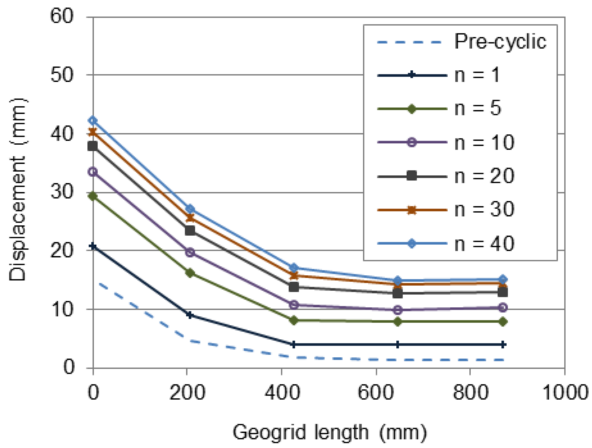

(b)

Figure 10. Pullout test results for A_F/P_R = 0.40 (I_D = 50%, P_S/P_R = 0.50, f = 0.1 Hz, n = 40): (a) evolution of pullout force with frontal displacement; (b) displacements recorded along the geogrid during the cyclic loading phase.

This manuscript is the accepted version of the paper:

HDPE geogrid-residual soil interaction under monotonic and cyclic pullout loading, Geosynthetics International, Vol. 27, Issue 1, pp. 79-96, https://doi.org/10.1680/jgein.19.00057

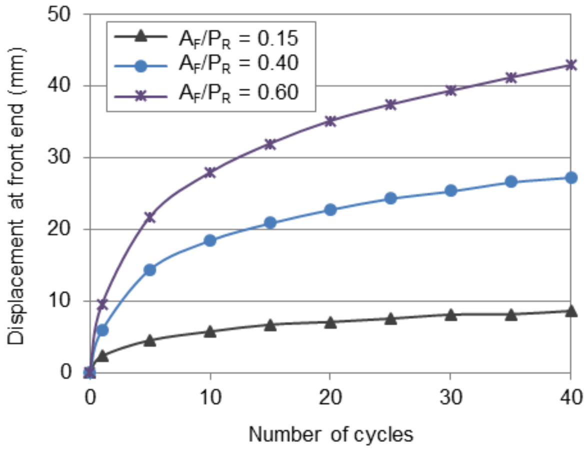

(a)

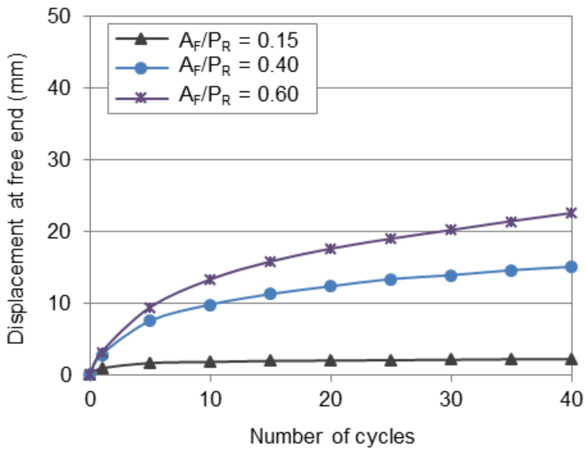

(b)

Figure 11. Influence of amplitude on the accumulated displacements at the geogrid ends during the cyclic loading phase (I_D = 50%, P_S/P_R = 0.50, f = 0.1 Hz, n = 40): (a) front end; (b) free end.

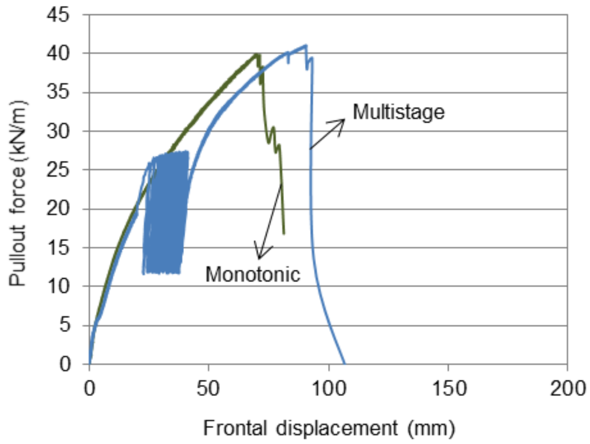

(a)

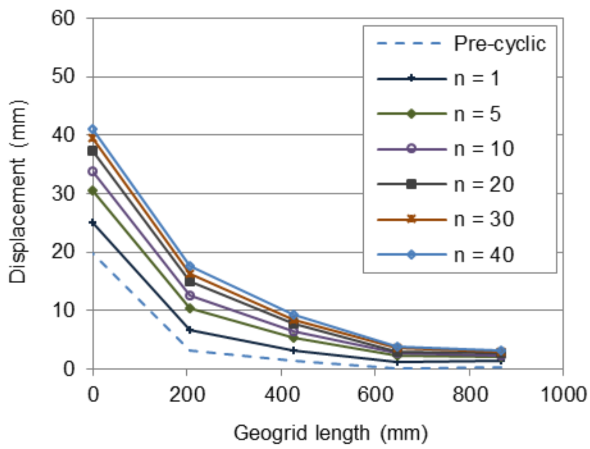

(b)

Figure 12. Pullout test results for A_F/P_R = 0.40 (I_D = 85%, P_S/P_R = 0.50, f = 0.1 Hz, n = 40): (a) evolution of pullout force with frontal displacement; (b) displacements recorded along the geogrid during the cyclic loading phase.

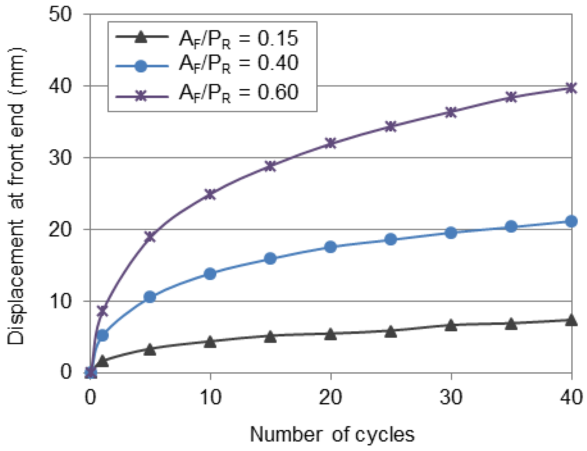

(a)

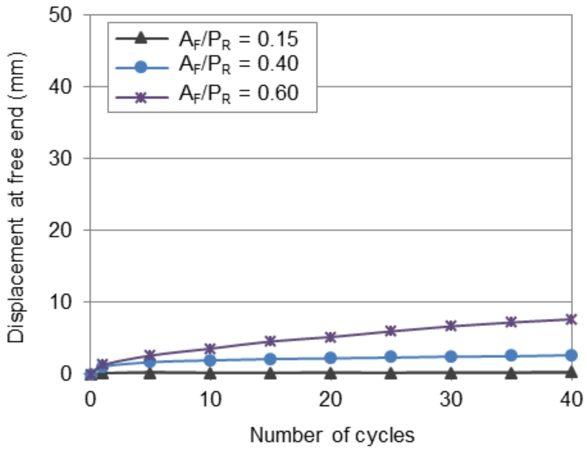

(b)

Figure 13. Influence of amplitude on the accumulated displacements at the geogrid ends during the cyclic loading phase (I_D = 85%, P_S/P_R = 0.50, f = 0.1 Hz, n = 40): (a) front end; (b) free end.

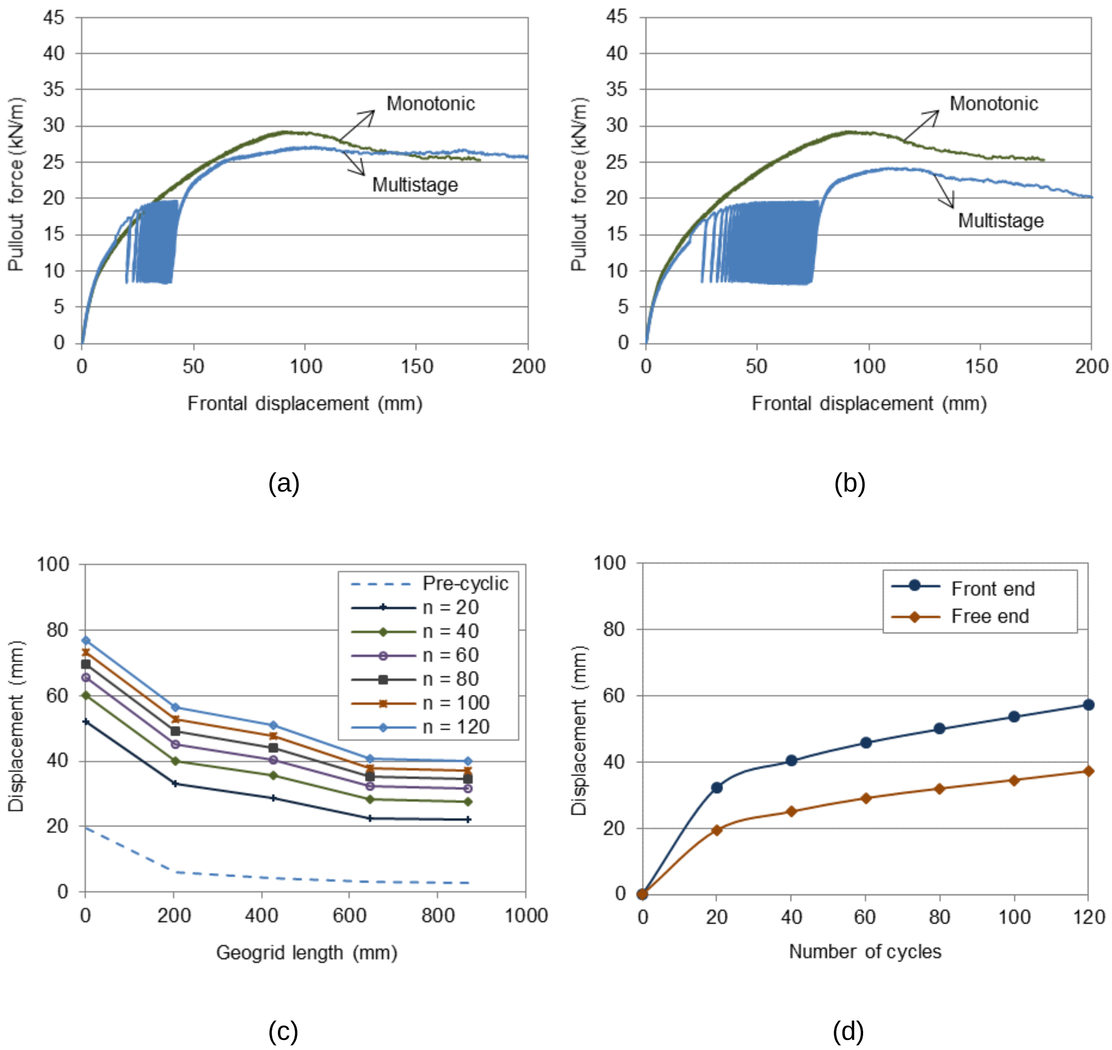

Figure 14. Influence of number of cycles on the pullout test results (I_D = 50%, P_S/P_R = 0.50, f = 0.1 Hz, A_F/P_R = 0.40): (a) evolution of pullout force with frontal displacement (n = 40); (b) evolution of pullout force with frontal displacement (n = 120); (c) displacements recorded along the geogrid during the cyclic phase (n = 120); (d) accumulated displacements at the geogrid ends (n = 120).

This manuscript is the accepted version of the paper:

HDPE geogrid-residual soil interaction under monotonic and cyclic pullout loading, Geosynthetics International, Vol. 27, Issue 1, pp. 79-96, https://doi.org/10.1680/jgein.19.00057

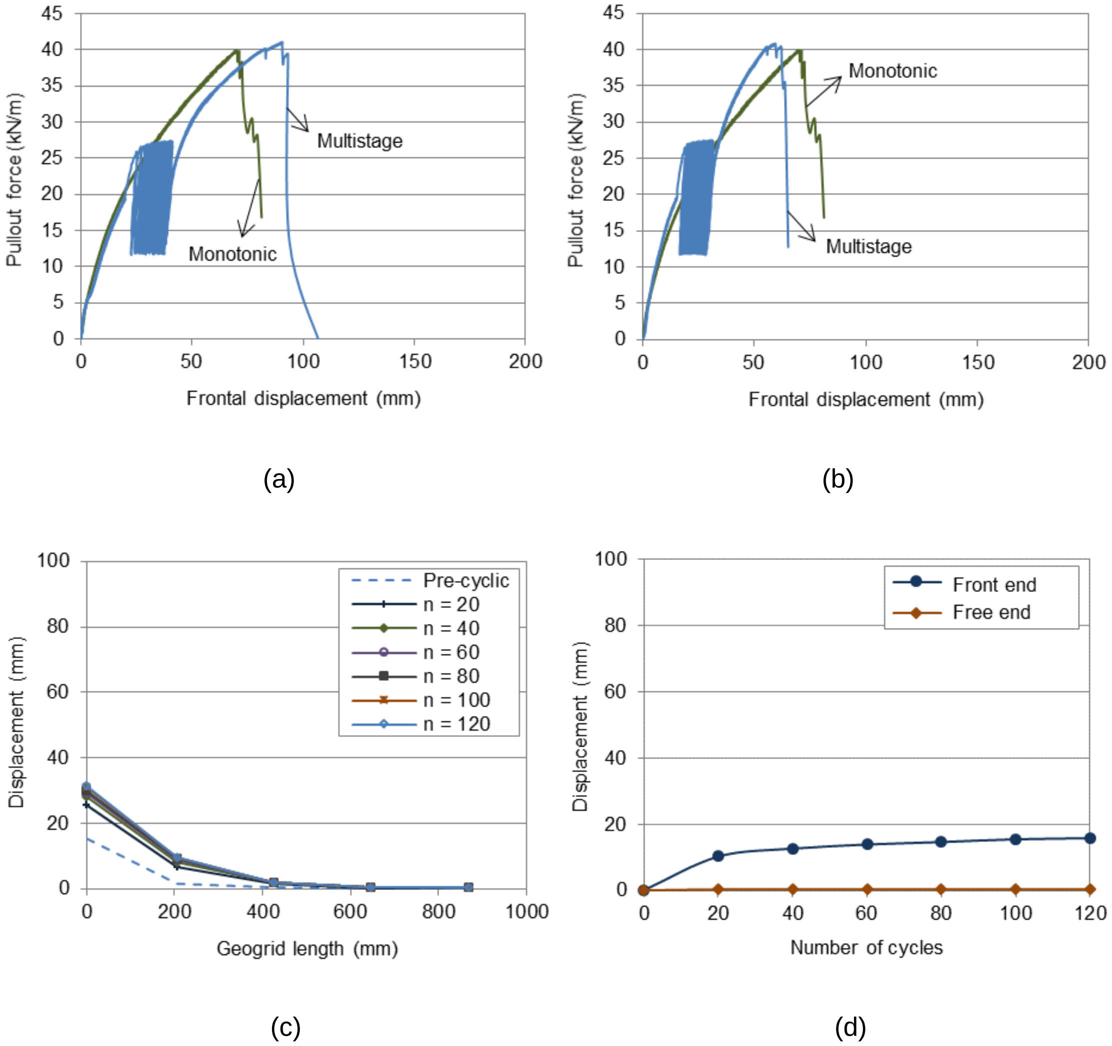

Figure 15. Influence of number of cycles on the pullout test results (I_D = 85%, P_S/P_R = 0.50, f = 0.1 Hz, A_F/P_R = 0.40): (a) evolution of pullout force with frontal displacement (n = 40); (b) evolution of pullout force with frontal displacement (n = 120); (c) displacements recorded along the geogrid during the cyclic phase (n = 120); (d) accumulated displacements at the geogrid ends (n = 120).